A Rapidly Activating and Slowly Inactivating Potassium Channel Cloned from Human Heart

Functional Analysis after Stable Mammalian Cell Culture Expression

DIRK J. SNYDERS, MICHAEL M. TAMKUN, and PAUL B. BENNETT

From the Departments of Medicine, Pharmacology, and Molecular Physiology and Biophysics, Vanderbilt University School of Medicine, Nashville, Tennessee 37232-2171

ABSTRACT The electrophysiological properties of HK2 (Kv1.5), a K^+ channel cloned from human ventricle, were investigated after stable expression in a mouse *Ltk*$^-$ cell line. Cell lines that expressed HK2 mRNA displayed a current with delayed rectifier properties at 23°C, while sham transfected cell lines showed neither specific HK2 mRNA hybridization nor voltage-activated currents under whole cell conditions. The expression of the HK2 current has been stable for over two years. The dependence of the reversal potential of this current on the external K^+ concentration (55 mV/decade) confirmed K^+ selectivity, and the tail envelope test was satisfied, indicating expression of a single population of K^+ channels. The activation time course was fast and sigmoidal (time constants declined from 10 ms to <2 ms between 0 and +60 mV). The midpoint and slope factor of the activation curve were $E_h = -14 \pm 5$ mV and $k = 5.9 \pm 0.9$ ($n = 31$), respectively. Slow partial inactivation was observed especially at large depolarizations (20 ± 2% after 250 ms at +60 mV, $n = 32$), and was incomplete in 5 s (69 ± 3%, $n = 14$). This slow inactivation appeared to be a genuine gating process and not due to K^+ accumulation, because it was present regardless of the size of the current and was observed even with 140 mM external K^+ concentration. Slow inactivation had a biexponential time course with largely voltage-independent time constants of ~240 and 2,700 ms between −10 and +60 mV. The voltage dependence of slow inactivation overlapped with that of activation: $E_h = -25 \pm 4$ mV and $k = 3.7 \pm 0.7$ ($n = 14$). The fully activated current–voltage relationship displayed outward rectification in 4 mM external K^+ concentration, but was more linear at higher external K^+ concentrations, changes that could be explained in part on the basis of constant field (Goldman-Hodgkin-Katz) rectification. Activation and inactivation kinetics displayed a marked temperature dependence, resulting in faster activation and enhanced inactivation at higher

Address reprint requests to Dr. Dirk J. Snyders, Stahlman Cardiovascular Research Program, MCN-CC-2209, Vanderbilt University School of Medicine, Nashville, TN 37232-2171.

J. GEN. PHYSIOL. © The Rockefeller University Press · 0022-1295/93/04/0513/31 $2.00
Volume 101 April 1993 513–543

temperature. The current was sensitive to low concentrations of 4-aminopyridine, but relatively insensitive to external TEA and to high concentrations of dendrotoxin. The expressed current did not resemble either the rapid or the slow components of delayed rectification described in guinea pig myocytes. However, this channel has many similarities to the rapidly activating delayed rectifying currents described in adult rat atrial and neonatal canine epicardial myocytes. Therefore human Kv1.5 may contribute to the initial fast repolarization and to the K^+ conductance during the plateau phase of the cardiac action potential.

INTRODUCTION

K^+ channels play important roles in cardiac excitability as they are involved in maintaining the resting potential, in early fast repolarization, in control of plateau and action potential duration, and in pacemaking activity (see Gintant, Cohen, Datyner, and Kline, 1991 for a review). However, detailed quantitative study of cardiac K^+ channels is complicated by the presence of multiple overlapping ionic currents in native cardiac myocytes. A combination of ion substitution and pharmacological dissection has been used to eliminate all but the current of interest (Balser, Bennett, and Roden, 1990; Sanguinetti and Jurkiewicz, 1990*a*). Although valuable, this procedure may introduce experimental difficulties: for instance, the use of divalent cations to block Ca^{2+} currents may modify gating properties of K^+ channels (Agus, Dukes, and Morad, 1991; Fan and Hiraoka, 1991; Follmer, Lodge, Cullinan, and Colatsky, 1992). In addition, kinetic analysis may be problematic if block of other currents by drugs is not time and voltage independent (Campbell, Qu, Rasmusson, and Strauss, 1993; Snyders, Bennett, and Hondeghem, 1991*a*).

Based on homology with *Shaker* K^+ channels (Papazian, Schwarz, Tempel, Jan, and Jan, 1987), several K^+ channels have recently been cloned from rat heart (Tseng-Crank, Tseng, Schwartz, and Tanouye, 1990; Paulmichl, Nasmith, Hellmiss, Reed, Boyle, Nerbonne, Peralta, and Clapham, 1991; Roberds and Tamkun, 1991*a*), and human heart (Tamkun, Knoth, Walbridge, Kroemer, Roden, and Glover, 1991). One of these human channels, designated HK2, was cloned from a human ventricular cDNA library. Analysis of tissue-specific expression indicated that this channel mRNA is expressed in the ventricle and more abundantly in the atrium (Tamkun et al., 1991). This human channel displays 86% overall homology with a channel cloned from rat heart (RK4) (Roberds and Tamkun, 1991*a*) and 96% identity in the central core region (containing the six membrane-spanning domains). Under a proposed nomenclature for cloned vertebrate K^+ channels (Chandy, 1991), these channels, although not identical, represent human and rat cardiac isoforms of Kv1.5.

The purpose of this study was to stably express this human cardiac K^+ channel in a mammalian cell line and to determine its functional characteristics in order to compare this current to the known phenotypes of time- and voltage-dependent K^+ currents in native myocytes. The expressed current displayed high K^+ selectivity, outward rectification, activation at depolarized potentials with fast activation kinetics, and slow inactivation. Therefore, this cloned channel may correspond to the very fast activating currents seen in rat atrial myocytes (Boyle and Nerbonne, 1991) and canine neonatal epicardial ventricular myocytes (Jeck and Boyden, 1992). Under the experimental conditions used in this study, no contaminating voltage-activated

currents were observed. In conjunction with the stable nature of the expression, this expression system provides an important new tool to study functional and pharmacological characteristics of cardiac ion channels (Snyders, Knoth, Roberds, and Tamkun, 1992*a*; Snyders, Roberds, Knoth, Bennett, and Tamkun, 1992*b*).

Preliminary results were presented at the 64th annual scientific meeting of the American Heart Association (Snyders, Knoth, Roberds, and Tamkun, 1991*c*).

METHODS

Transfection and Cell Culture

The SphI-EcoRV fragment (basepairs 161–2059) of the HK2 cDNA (Tamkun et al., 1991) was blunted with Klenow and subcloned in the EcoRV site of pMSVNeo (Chung, Wang, Potter,

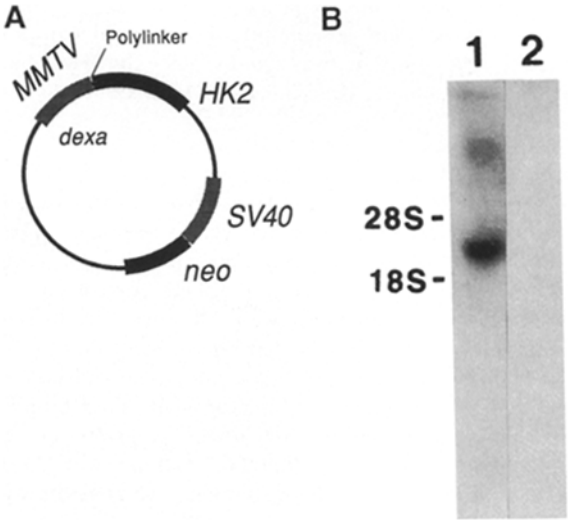

FIGURE 1. Transfection vector and mRNA expression. (*A*) Diagram of pMSVneo vector. *MMTV,* murine mammary tumor virus promotor; *dexa,* dexamethasone; *SV40,* simian virus SV40 early promotor; *neo,* neomycin resistance gene; *HK2,* coding sequence for HK2 K^+ channel, inserted at the polylinker site. The constitutively active SV40 promoter confers neomycin resistance to cells that successfully incorporate the construct, allowing them to survive under continuous G418 selection. Channel expression is activated by dexamethasone induction of the MMTV promotor. The construct for sham transfection lacked the HK2 coding sequence. (*B*) High stringency Northern analysis of a HK2 transfected cell line (lane *1*) and a sham transfected cell line (lane *2*) after induction with 1 μM dexamethasone for 24 h. 10 μg of total L cell RNA was fractionated by formaldehyde gel electrophoresis and hybridized as described previously (Tamkun et al., 1991). Ethidium bromide staining confirmed that equal amounts of intact RNA had been loaded on the agarose gel. The hybridization probe was the full-length HK2 cDNA. The specific band of the appropriate size for HK2 message was only detected in the HK2 transfected cell line (lane *1*).

Venter, and Fraser, 1988). This vector contains the dexamethasone-inducible murine mammary tumor virus promoter controlling transcription of the cDNA inserted at the polylinker site, and a gene conferring neomycin resistance driven by the SV40 early promoter (Fig. 1 *A*). The HK2-pMSVNeo construct contained the entire coding sequence and in addition 22 and 59 bp of the 5′ and 3′ untranslated sequence, respectively. The cDNA-containing expression vector was transfected into mouse *Ltk*⁻ cells (L cells) using the calcium phosphate method as described previously (Takeyasu, Tamkun, Siegel, and Fambrough, 1987). After 24 h, selection with 0.5 mg/ml G418 (a neomycin analogue) was initiated for 2 wk or until discrete foci formed.

Individual foci were isolated, maintained in 0.25 mg/ml G418, and screened for HK2 mRNA expression by Northern analysis as previously described (Tamkun et al., 1991). Specific hybridization was obtained in each of 10 cell lines randomly selected from the 30 foci surviving G418 selection. Two of these positive cell lines were assayed for functional current expression, which was indistinguishable, and one (L-HK2.7) was chosen for further study. Cell lines transfected with the same vector, but lacking the HK2 cDNA, were prepared in parallel and served as negative controls (sham transfected cell lines). The sham transfected cells did not display specific mRNA hybridization on Northern analysis at high stringency with a HK2-specific probe (Fig. 1 *B*) and did not express HK2 currents (see Results).

Cells were cultured in DMEM supplemented with 10% horse serum and 0.25 mg/ml G418 under a 5% CO_2 atmosphere. The cultures were passed every 4–5 d using a brief trypsin treatment. Before experimental use, subconfluent cultures were incubated with 2 μM dexamethasone for 24 h to induce efficient channel expression. The cells were removed from the dish with a rubber policeman, a procedure that left the majority of the cells intact. The cell suspension was stored at room temperature and used within 12 h for all the experiments reported here. However, up to 24 h of storage at room temperature did not yield significantly different results. Trypsin treatment of the cells before use was avoided since the HK2 channel has six potential tryptic cleavage sites on its presumed extracellular face (Tamkun et al., 1991).

Electrical Recording

Recordings were made with an Axopatch-1A patch clamp amplifier (Axon Instruments, Inc., Foster City, CA) using the whole cell configuration of the patch clamp technique (Hamill, Marty, Neher, Sakmann, and Sigworth, 1981). Micropipettes were pulled from starbore borosilicate glass (Radnoti Co., Monrovia, CA) and were heat polished. All currents were recorded at room temperature (21–23°C) unless indicated otherwise. The current records were sampled at 3–10 times the anti-alias filter setting, stored on the hard disk of an IBM PC-AT for subsequent analysis, and archived on optical disk. Data acquisition and command potentials were controlled by a versatile custom-made programmable stimulator. Gain, filter frequency, and temperature were stored with each record. To ensure voltage clamp quality, electrode resistance was kept below 3.5 MΩ; the average resistance was 2.2 ± 0.5 MΩ (n = 46). Junction potentials were zeroed with the electrode in the standard bath solution. The electrodes were gently lowered onto the cells and gigaohm seal formation was achieved by suction (17 ± 9 GΩ; range 5–50 GΩ).

After establishing the whole cell configuration, the capacitive transients elicited by symmetrical 10-mV voltage clamp steps from −80 mV were recorded at 50 kHz (filtered at 10 kHz) for subsequent calculation of capacitive surface area, access resistance, and input impedance (Fig. 2). Thereafter, capacitance and series resistance compensation were optimized and 80% compensation was usually obtained. With an average current of 1.6 nA at +60 mV (i.e., worst case analysis of largest currents associated with strongest depolarization), no significant voltage errors (<5 mV) due to series resistance were expected with the electrodes used, and this was confirmed by the calculated access resistance (R_a) (Table I). Fig. 2 illustrates that, compared with ventricular myocytes, the low capacitance enabled fast clamp control: τ = 45–200 μs before compensation (Table I), which improved further after compensation.

Solutions

The intracellular pipette filling solution contained (mM): 110 KCl, 10 HEPES, 5 K_4BAPTA, 5 K_2ATP, and 1 $MgCl_2$, and was adjusted to pH 7.2 with KOH, yielding a final intracellular K^+ concentration of ~145 mM. The bath solution contained (mM): 130 NaCl, 4 KCl, 1.8 $CaCl_2$, 1 $MgCl_2$, 10 HEPES, and 10 glucose, and was adjusted to pH 7.35 with NaOH. To obtain higher

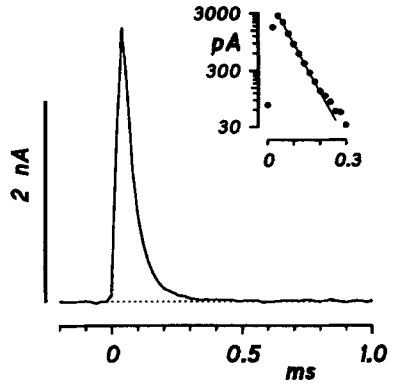

FIGURE 2. Passive properties. The capacitive transient for a 10-mV depolarization from −80 to −70 mV is shown after linear leak subtraction. Numerical integration of the area under the curve yielded a capacitance of 21 pF. The time constant of the falling phase was 52 μs (semilogarithmic graph in inset). Calculated uncompensated access resistance was 2.5 MΩ. Data were sampled at 50 kHz and filtered at 10 kHz.

extracellular K^+ concentrations, equimolar substitution of KCl for NaCl was used. Tetraethylammonium (TEA) and 4-aminopyridine (4-AP) were added to the extracellular solution as needed, and for concentrations >5 mM, equimolar substitution with NaCl was used. All these chemical compounds were obtained from Sigma Chemical Co. (St. Louis, MO).

Dendrotoxin (DTX-I) was kindly provided by Dr. R. Hartshorne (Oregon Health Sciences University, Portland, OR). DTX-I was purified as described previously (Benishin, Sorensen, Brown, Krueger, and Blaustein, 1988). Because dendrotoxin did not block this channel in concentrations up to 100 nM, the following controls were done: after superfusion with DTX-I for 10–15 min, the perfusion was switched to 75 mM extracellular K^+ to confirm that the solution switch had been complete within 2–3 min, as assessed by the change in the reversal potential. Biological activity of this DTX-I lot was confirmed by ^{125}I-DTX-I binding to brain synaptosomes and by full suppression of Kv1.1 (RK1) current in transfected L cells with only 5 nM DTX-I. The latter is consistent with the high affinity of Kv1.1 for DTX (Stühmer, Stocker, Sakmann, Seeburg, Baumann, Grupe, and Pongs, 1988; Hurst, Busch, Kavanaugh, Osborne, North, and Adelman, 1991).

Pulse Protocols and Analysis

The holding potential was −80 mV unless indicated otherwise. Repriming kinetics of HK2 (deactivation and recovery from slow inactivation; see Results) were sufficiently fast to allow for pulse trains up to 0.5 Hz without decrement of the current (250-ms pulses). However, to ensure identical conditions throughout the protocols, the cycle time was 10 s or slower (with the exception of specific pulse trains). In the case of drug application or changes in external K^+

TABLE I

Properties of the L Cell Expression System

	Size	SA	C_m	C_m/SA	R_{ME}	τ_c	R_a	I_{60}	I_{60}/C_m	I_{60}/SA
	μm	*μm²*	*pF*	*pF/μm²*	*MΩ*	*μs*	*MΩ*	*nA*	*pA/pF*	*pA/μm²*
Mean	16.0	813	18.3	2.2	2.2	114	6.6	1.6	92	2.0
SD	1.3	129	5.2	0.5	0.5	53	3.1	1.2	61	1.4
N	46	46	40	40	46	40	40	40	40	40

Size: cross-sectional diameter, measured with eyepiece micrometer at ×40. SA: surface area, calculated assuming smooth spherical shape. C_m: cell capacitance obtained by integration of uncompensated capacitive transients (see Methods). τ_c: time constant of uncompensated capacitive transient. R_{ME}: electrode DC resistance. R_a: uncompensated access resistance ($R_a = \tau_c/C_m$). I_{60}: maximum current at +60 mV.

concentration, the change in solution was monitored with test pulses from −80 to +50 mV, applied every 15 or 30 s until steady state was obtained.

The protocol to obtain current–voltage relationships and activation curves consisted of 250-ms pulses that were imposed in 10-mV increments between −80 and +60 mV, with additional interpolated pulses to yield 5-mV increments between −30 and +10 mV (activation range of HK2). The steady-state current–voltage relationships were obtained by measuring the current at the end of the 250-ms depolarizations. Between −80 and −40 mV, only passive linear leak was observed; least-squares fits to these data were used for passive leak correction. Capacitive transients were subtracted using an appropriately scaled average of 16–32 hyperpolarizing pulses from −80 to −100 mV. Deactivating tail currents were recorded at −30 or −50 mV. The activation curve was obtained from the tail current amplitude immediately after the capacitive transient, or from the amplitude of the exponential fit to its time course: both gave similar results. For steady-state curves, raw data points were averaged over a small time window (2–5 ms). Peak currents were obtained from the best second-order polynomial fit to the raw data points using a moving window of 10–20 ms, as used previously for analyzing I_{Na} (Snyders and Hondeghem, 1990). Raw tracings shown in this paper were corrected for linear leak and capacitive transients as described above and digitally filtered at 2 kHz in the frequency domain after Fourier transformation.

The voltage dependence of channel opening or inactivation (activation and inactivation curves) was fitted with a Boltzmann equation $y = 1/\{1 + \exp[-(E - E_h)/k]\}$, where k represents the slope factor and E_h the voltage at which 50% of the channels are open or inactivated. Because inactivation was usually incomplete, data were normalized after subtraction of the noninactivating fraction at the test potential. The time courses of tail currents and slow inactivation were fitted with a sum of exponentials. Activation kinetics were fitted with a single exponential to the latter 50% of activation (White and Bezanilla, 1985; Spires and Begenisich, 1989) (dominant time constant of activation), or with an equation of the form $[1 - A \times \exp(-t/\tau_n)]^n$, with $n = 4$ to reflect independent activation of four subunits (Koren, Liman, Logothetis, Nadal-Ginard, and Hess, 1990; Zagotta and Aldrich, 1990; MacKinnon, 1991). The curve-fitting procedure used a nonlinear least-squares (Gauss-Newton) algorithm; results were displayed in linear and semilogarithmic format together with the difference plot. Goodness of the fit and required number of exponential components were judged by comparing χ^2 values statistically (F test) and by inspection for systematic, nonrandom trends in the difference plot (see Fig. 8 *C*).

Results are expressed as mean ± SD. Analysis of variance with appropriate post hoc comparisons was used to compare the differences in mean values; $P < 0.05$ was considered significant.

RESULTS

Expressed HK2 Current

Fig. 3 *A* shows recordings from a mouse L cell expressing HK2. Tracings for depolarization from −80 mV to potentials between −100 and +60 mV were superimposed from comparison. Between −100 and −30 mV, no voltage activated current was observed. With further depolarization, a progressively larger outward current was recorded. The activation of the current proceeded with a sigmoidal time course, and the rate of activation increased with depolarization. At the most positive voltages, the current declined ~10% during depolarization maintained for 250 ms. This slow inactivation is analyzed in more detail below. Upon repolarization to −30 mV, outward tail currents were recorded. In this cell, the size of the expressed current

at +50 mV was 1,320 pA or 87 pA/pF. Average values at +60 mV were 1.6 ± 1.2 nA or 92 ± 60 pA/pF (n = 40).

Without induction of the transfected cells, these typical HK2 whole cell currents were not observed. After 8–24 h induction with 2 μM dexamethasone, outward currents ranging from 0.5 to 20 nA were obtained at +50 mV. Because of inherent series resistance problems associated with higher current densities, the latter value (20 nA at +50 mV) should only be considered an approximate indication of the highest levels of expression; cells that expressed these current densities were not used for further analysis.

Stable Transfection and Electrophysiological Properties of L Cells

Sham transfected cells (cell lines that underwent the full transfection procedure with a pMSVneo vector lacking the HK2 coding sequence; see Methods) did not display

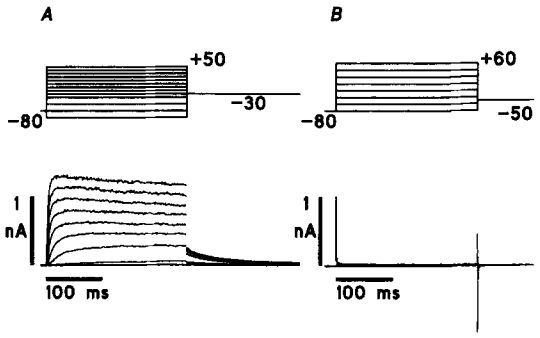

FIGURE 3. HK2 currents expressed in a mouse L cell compared with sham transfected cells. (*A*) HK2 transfected cell. Superimposed current tracings for depolarizations from a holding potential of −80 mV to voltages between −100 and +50 mV (*top*); tail currents were obtained at −30 mV. Tracings for −100 to −30 mV all superimpose (*lowermost tracing*). Linear leak (3.1 GΩ) and capacitive transients were subtracted as described in Methods. Data were sampled at 10 kHz and filtered at 5 kHz (4-pole Bessel filter). Cell capacitance 15.1 pF; size 15 μm; resting potential −28 mV. (*B*) Sham transfected cell. Tracings are shown for depolarization from −80 mV to voltages up to +60 mV in 20-mV increments (*inset*). Raw tracings are displayed without subtraction of linear leak or capacitive transients. The current–voltage relationship was linear from −80 to +60 mV with 5.1 GΩ input impedance.

specific mRNA hybridization on Northern analysis at high stringency with a HK2-specific probe (Fig. 1 *B*). No voltage-gated K^+ channels were observed in these cells (Fig. 3 *B*) under the recording conditions used in this study (n = 6). Only a time-independent leak current was observed, which was linear between −100 and +40 mV and reversed close to 0 mV. This current was typically less than −80 pA at the holding potential of −80 mV, indicating a whole cell impedance > 1 GΩ. At +50 and +60 mV a small additional outward current was occasionally observed. This current was < 3 pA/pF or 40 pA/cell, or < 2% of typical whole cell HK2 current. Sham transfected cells (either induced or not) or noninduced L-HK2.7 cells displayed low resting potentials (−6 mV or less). In contrast, the HK2 transfected cells had a resting potential of −29 ± 6 mV (n = 26) 24 h after induction of HK2 expression. No sodium or calcium currents were observed in either sham or truly transfected cell

lines ($n > 300$). Average values for cell size, capacitance, and access resistance are provided in Table I.

Envelope of Tails Test

If the expressed current represents a single homogenous class of channels, then the magnitude of the deactivating tail currents should be proportional to the current activated during the depolarizing test pulse eliciting those tails (Hodgkin and Huxley, 1952). Fig. 4 shows the results of this envelope of tails test. The activation time course during the depolarization to 0 mV was sufficiently slow to easily obtain tail currents in conditions where the current during depolarization changed about fivefold. Fig. 4 *A* shows that the tail current amplitude indeed rose up to 150 ms and then tapered off slightly, as did the current recorded during depolarization to 0 mV.

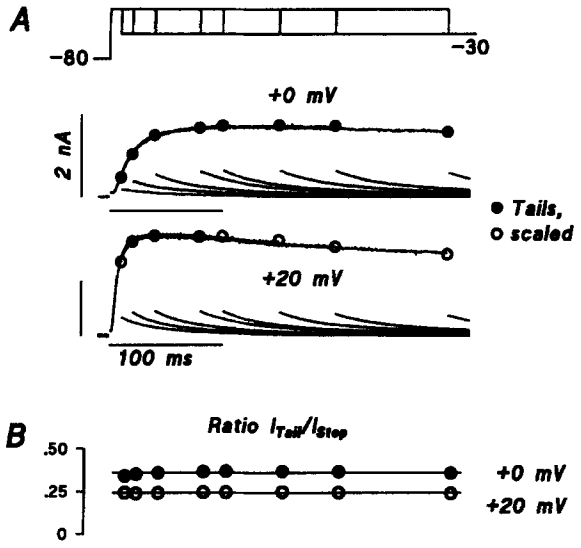

FIGURE 4. Envelope of tails test. (*A*) Superimposed tracings of currents obtained during depolarization (0 and +20 mV), and subsequent tail currents. Symbols superimposed on the current during the step indicate the scaled tail amplitude using a single scaling factor (2.75 for 0 mV, 4.1 for +20 mV). Pulse protocol (*top*): a variable duration depolarization to 0 mV or +20 mV was followed by a step to −30 mV for tail current measurement. Holding potential −80 mV. Residual uncompensated access resistance was 1.2 MΩ. (*B*) Ratio of tail current amplitude (I_{tail}) and current activated during depolarization (I_{step}). The horizontal line is a linear fit to the data points with the following parameters. For depolarization to 0 mV: intercept 0.36, slope 2×10^{-5}/ms, $r = 0.34$; for depolarization to +20 mV: intercept 0.24, slope 3×10^{-5}/ms, $r = 0.07$ (i.e., not correlated with time in either case).

These results were quantitated in two ways. In Fig. 4 *A*, the tail current measured after the longest step to 0 mV was scaled to match the current at the end of the preceding depolarizing test pulse. This scaling factor (2.75 in this example) was then applied to all other tail currents, and the resulting values are indicated by the circles. These points all superimposed on the tracing during depolarization, indicating that the test was satisfied. This was confirmed by the more stringent test shown in Fig. 4 *B* (Sanguinetti and Jurkiewicz, 1990*a*). For each test depolarization, the ratio of the tail current size (I_{tail}) to the amount of current activated during the eliciting depolarization (I_{step}) was obtained and displayed as a function of the duration of the

corresponding depolarization (filled symbols). This ratio was independent of time and current size. The bottom part of Fig. 4 *A* shows the results obtained in the same cell at +20 mV and illustrates that the test remained satisfied during the slow inactivation phase (open symbols in Fig. 4 *A*). The latter was confirmed by the ratio analysis (4 *B*, open symbols). Similar results were obtained in five other cells for different combinations of step and tail potential (Table II) in which the tail envelope test remained satisfied during the slow inactivation at large depolarizations as well.

Potassium Selectivity

The increase of current with depolarization, and the outward tails at −50 and −30 mV (Fig. 3) are consistent with the behavior of a K^+ channel. To test whether K^+ was indeed the main charge carrier and to determine the selectivity of this channel, reversal potentials were obtained in different external K^+ concentrations. The current was fully activated using a 25-ms depolarization to +50 mV, and the

TABLE II

Envelope Tail Current Ratio

Experiment	E1/E2	Expected ratio	Observed ratio*	Observed/ expected
910125a-5	0/−30	.62	.360 ± .009	.48
910125a-6	30/−30	.50	.244 ± .003	.58
911127a-13	10/−50	.33	.18 ± .01	.54
911127c-2	10/−50	.33	.201 ± .009	.61
911204a-8	0/−50	.37	.17 ± .01	.46
911204b-7	0/−50	.37	.13 ± .02	.35
911204c-12	0/−40	.50	.303 ± .004	.60
911204c-13	30/−40	.33	.170 ± .005	.51

E1: step potential. E2: tail potential. Expected ratio: calculated from $(E2 - E_{rev})/(E1 - E_{rev})$, using −80 mV for E_{rev}.

*Mean ± SD (n = 7–10).

subsequent tail current amplitudes were measured at potentials between −110 and +40 mV. Because of the fast deactivation kinetics negative to −60 mV, the tail current amplitudes at these voltages were obtained from the amplitude of exponential fits to the time course. The reversal potential was obtained from a linear fit to the values obtained at four or five voltages bracketing the reversal potential (5-mV intervals). Average values were (extracellular $[K^+]$ in parenthesis): −81 ± 3 mV (4 mM, n = 6), −49 ± 2 mV (16 mM, n = 3), −13 ± 4 mV (75 mM, n = 3), and +7 mV (140 mM, n = 2). Fig. 5 shows the dependence of the reversal potential on the external K^+ concentration. The solid line represents the fitted Nernst equation (see legend). The resulting slope factor of 55 mV/decade indicated that the HK2 encoded channel was indeed highly selective for K^+. A fit of these data with the Goldman-Hodgkin-Katz voltage equation (Goldman, 1943; Hodgkin and Katz, 1949) yielded a relative selectivity (P_{Na}/P_K) of 0.007 ± 0.001.

Current–Voltage Relationship and Rectification

Fig. 6 *A* shows the current–voltage relationships for the maximum current during a 250-ms depolarization and the instantaneous (fully activated) current–voltage relationship. The current–voltage curves have been corrected for passive background leak as described in Methods. This current–voltage relationship illustrates that the current is activated at voltages positive to −30 mV. Before leak subtraction, the current–voltage curve crossed the zero-current axis at −29 mV, corresponding to the resting potential of this cell measured in current clamp mode (−28 mV). The sigmoidicity between −30 and +10 mV reflects the voltage dependence of channel opening (see below). Positive to 0 mV, the relationship was nearly linear. However, this quasi-linear section did not extrapolate to the reversal potential of the current, but to −26 mV. This is suggestive of outward rectification. Another indicator of outward rectification was provided by the analysis of the ratio of tail to step current in the envelope of tails test. As shown in Table II, this ratio was systematically lower than the ratio expected for a K^+-selective channel with ohmic (linear) conductance.

To evaluate the rectification properties, the instantaneous fully activated current–

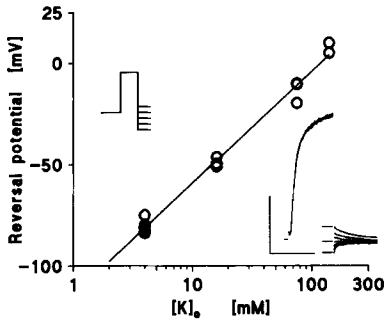

FIGURE 5. K^+ selectivity. The pulse protocol is shown in the inset on the left. The inset on the right shows tracings obtained in 4 mM external K^+. Calibration, 20 ms and 500 pA. The horizontal bars indicate, from top to bottom, the initial size of the tail current at −50, −80, and −110 mV. The solid line represents the fit of the Nernst equation $E_{rev} = A \times \log([K^+]_o/[K^+]_i) + V_{offs}$, with A = 55.1 mV and V_{offs} = 4.8 mV.

voltage relationship of HK2 was determined. In the example of Fig. 6 *A* (filled circles), this curve was obtained from tail currents after a short depolarizing step to +50 mV by extending the protocol of Fig. 5 to more positive potentials. The upward curvature in Fig. 6 *A* indicates that the HK2 current displayed outward rectification. The solid line represents a fit with using the constant field current equation (Goldman, 1943; Hodgkin and Katz, 1949).

Because constant field rectification depends on permeant ion concentration, the effect of varying external K^+ concentration was determined. In the experiment shown in Fig. 6 *B*, the instantaneous current–voltage relationships were obtained from tail current amplitudes at voltages negative to −30 mV (as in Figs. 5 and 6 *A*). At more positive potentials data were obtained from peak currents during depolarizing steps. In the voltage range between −30 and +10 mV, the currents from either protocol were corrected for the degree of partial activation or deactivation. Both methods to obtain this instantaneous current–voltage relationship gave similar results. Fig. 6 *B* shows that the outward rectification of HK2 indeed depended on the external K^+ concentration. Rectification was less pronounced at higher external K^+ concentra-

tions. With 75 mM (Fig. 6 *B*) and 140 mM external K^+ (other experiments) the relationship was almost linear. The solid lines in Fig. 6 *B* represent the fit of the constant field current equation to these data (see Discussion). The fitted value for the K^+ premeability (P_K) in 4 mM $[K^+]_o$ in this experiment was 5×10^{-8} s/cm.

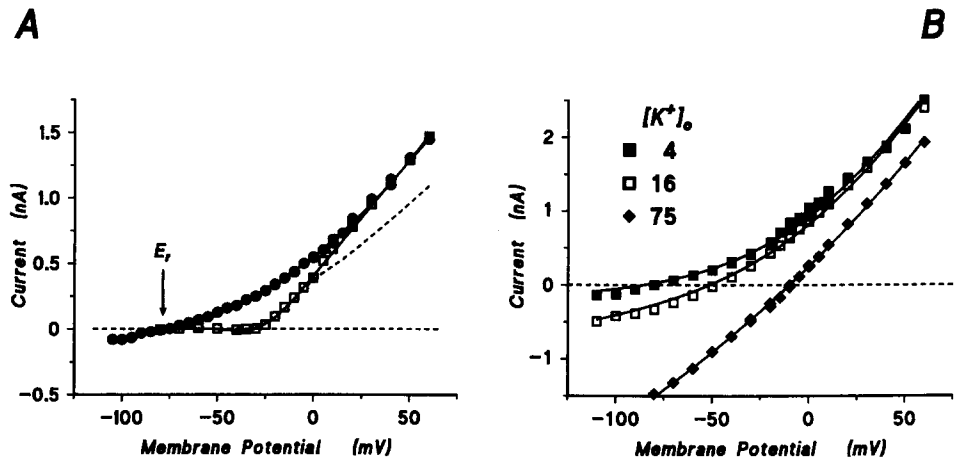

FIGURE 6. HK2 current–voltage relationships. (*A*) Current–voltage relationships. Maximum current attained during depolarization indicated by open squares. The dashed line represents current at the end of the 250-ms depolarizations. The difference between both curves is the amount of slow inactivation within 250 ms. The solid circles represent the fully activated current–voltage relationship. Instantaneous tail current amplitudes were obtained at different voltages after a 25-ms prepulse to +50 mV (protocol from Fig. 4). Current tracings were corrected for linear leak, and tail current amplitude was determined using exponential fits to the decaying current. The solid line was drawn according to the constant field current equation $I = P_K \times z \times F \times E \times \alpha \times \{[K^+]_i/(1 - \exp(-\alpha \times E)) + [K^+]_o/(1 - \exp(\alpha \times E))\}$ with $\alpha = (z \times F)/(R \times T)$. R, T, F, and z have their usual meaning; subscripts i and o indicate inside and outside concentrations, respectively; I is current density (per unit surface area); P_K represents the K^+ permeability. (*B*) Dependence of the fully activated current–voltage relationship on $[K^+]_o$, obtained in another cell at three K^+ concentrations. For negative potentials, data were obtained as in *A*. Positive to −20 mV, the fully activated current was obtained from the maximum current during depolarization, with corrections for the degree of activation (see Methods). The solid lines are drawn according to the constant field equation, with $P_K = 5 \times 10^{-8}$ cm/s for 4 mM. Relative values for 4, 16, and 75 mM were 1, 1.05, and 0.90, respectively.

Activation Curve and Activation Kinetics

Because of the nonlinear instantaneous current–voltage relationship, the voltage dependence of HK2 activation was obtained from the deactivating tail current amplitude at −50 mV (or −30 mV) as shown in Fig. 7 *A* after normalization to averaged maximum tail current (filled circles). Average values for the midpoint and slope factor from Boltzmann fits to these activation curves were $E_h = -14 \pm 4$ mV and $k = 5.9 \pm 0.9$ ($n = 31$). A similar voltage dependence of channel opening was obtained using the normalized permeability approach (P/P_{max}, open circles), in which

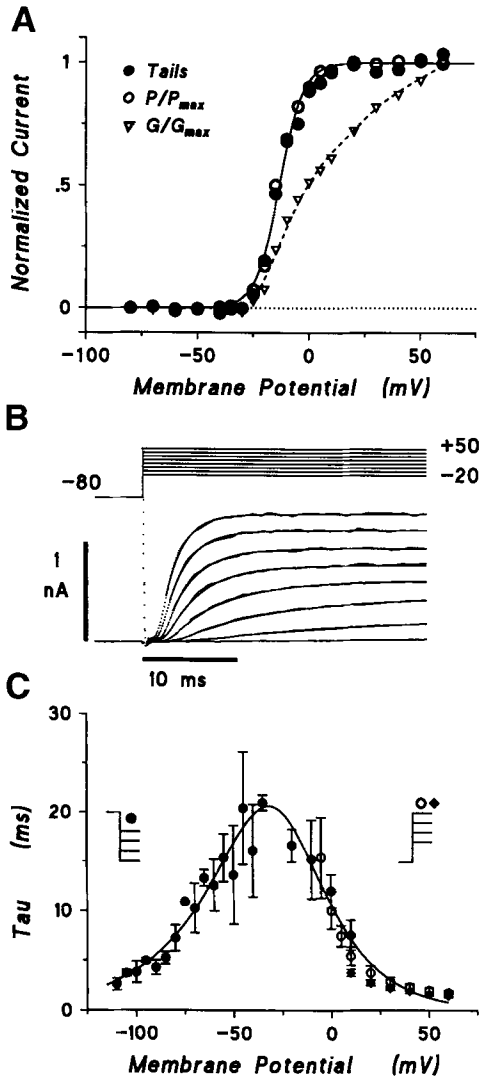

FIGURE 7. Activation curve and activation kinetics. (*A*) Quasi-steady-state activation curve obtained from tail current amplitude at −30 mV after 250-ms depolarizing steps to potentials between −80 and +60 mV (*filled circles*). The solid line represents the fit of the Boltzmann equation with the following parameters: midpoint −13 mV, slope factor 5.3 mV. Open circles represent the activation curve obtained with the normalized permeability method (peak current–voltage divided by fully activated current–voltage). The triangles and dashed line show the normalized conductance for the same experiment, using a reversal potential of −80 mV. A Boltzmann fit through these points yielded a midpoint of −2 mV and a slope factor of 13 mV. (*B*) Sigmoidal time course of channel opening. Raw current tracings for depolarizations to voltages between −20 and +50 mV in 10-mV increments. Monoexponential fits are superimposed (*solid line*). Digital subtraction of linear leak and capacitive transient. (*C*) Voltage dependence of activation and deactivation time constants. Time constants at positive potentials were obtained from the time course of current during depolarization using exponential fits (*open circles*) or the $n = 4$ model (*diamonds*). At negative potentials the time constant (*filled circles*) was obtained from exponential fits to the deactivating tail currents (as in Fig. 5, *inset*). Negative to −50 mV a single exponential was used. Between −20 and −40 mV double exponential fits were superior. The fast time constant is displayed.

the current at each voltage (Fig. 6 *A*) was normalized to the instantaneous maximum value at that voltage (Fig. 6 *B*). The dashed line in Fig. 7 *A* represents the normalized conductance $G(E)/G_{max} = I(E)/(E - E_{rev})$ for the same experiment. The voltage dependence determined in this way was more shallow than with both the tail current and P/P_{max} methods, as expected because of the nonlinear instantaneous current–voltage relationship.

The current activated after a delay, which resulted in a sigmoidal time course of the activation (Fig. 7 *B*). We attempted to fit this time course with the equation $I(t) = I_{max} \times [1 - \exp(-t/\tau_n)]^n$, in which the value of n was set to 4, reflecting the assumed four-subunit composition of the channel (MacKinnon, 1991). The voltage dependence of the activation time constants obtained in this way are shown as the solid diamonds in Fig. 7 *C*. However, the initial delay of the activation time course was poorly fitted at any potential, especially between −30 and +10 mV, which may have distorted the time constants. Therefore an alternate procedure was also used, in which the latter part of the activating current was fitted with a single exponential to obtain the dominant time constant of activation (White and Bezanilla, 1985; Spires and Begenisich, 1989). In addition, this allowed for comparison with results obtained for other homologous channels. This approach yielded very similar results over the voltage range between +20 and +60 mV, but differed at lower voltages (Fig. 7 *C*, open circles). Because no current activated at voltages negative to −30 mV, time constants were obtained from deactivating tail currents at potentials between −30 and −110 mV (indicated by the solid circles in Fig. 7 *C*).

Slow Inactivation

As shown in Figs. 3 and 8 *A*, slow partial inactivation was observed at large depolarizations. After 250 ms at +60 mV, the current was reduced by 20 ± 2% (n = 31) compared with the early peak current. This slow inactivation was more pronounced at the larger depolarizations (Fig. 3), and was incomplete even when the test pulse duration was increased to 5 s (69 ± 3% inactivation; Fig. 8 *A*). This slow inactivation was independent of the size of the expressed K^+ current, and was observed with all external K^+ concentrations tested (4–140 mM), indicating that it represented a genuine gating property.

The voltage dependence of slow inactivation (Fig. 8 *B*) overlapped with that of activation: the midpoint and slope factor obtained from Boltzmann fits were E_h = −25 ± 4 mV and k = 3.7 ± 0.4 (n = 14), respectively. In eight experiments, the average difference between the midpoints for activation and inactivation was 8.6 ± 0.8 mV ($P < 0.05$). The time course of slow inactivation was fitted by a sum of exponentials. With 5-s depolarizing pulses, two exponential components could be resolved (Fig. 8 *C*). One component had a time constant of 200–300 ms, while the slower component had a time constant of 2–3 s. In contrast to the marked voltage dependence of the activation kinetics, both the fast and the slow time constants of inactivation displayed only a weak voltage dependence (Fig. 8 *D*). The relative contribution of the fast and slow components was also almost independent of membrane potential (Fig. 8 *E*). In four additional experiments, slow inactivation was not complete even with 30- and 45-s depolarizations (30 s: 86 ± 1% inactivation, n = 3). In all experiments, the voltage dependence of inactivation overlapped with the threshold for channel opening, such that inactivation was observed only if at least a small degree of channel opening had occurred.

Monoexponential analysis of recovery from inactivation (after a 5-s depolarization to +50 mV) indicated a time constant of 1,650 ± 110 ms (n = 3) at −50 mV. However, with brief depolarizations (up to 250 ms), no decline of outward current was observed at stimulation rates up to 0.5 Hz (holding potential −80 mV, n = 5).

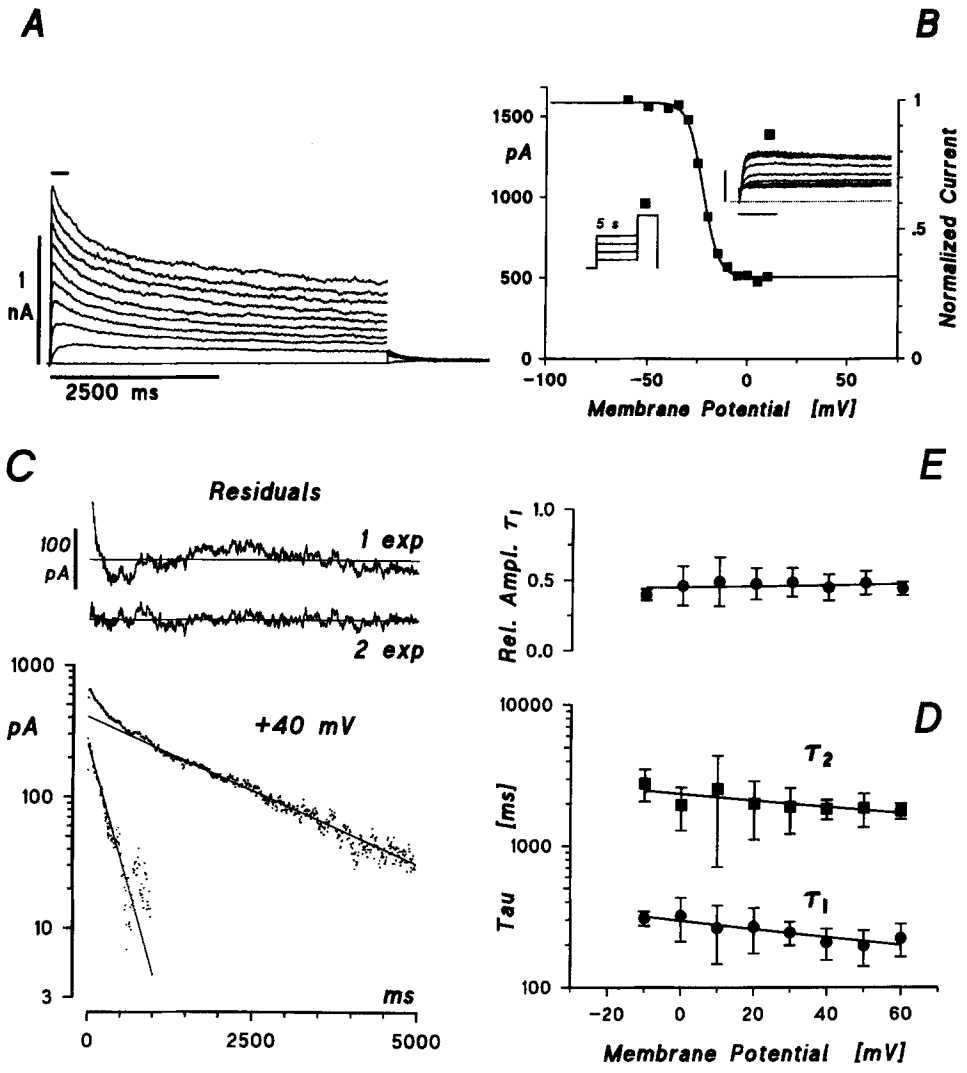

FIGURE 8. Slow inactivation. (*A*) Superimposed recordings for 5-s depolarizations from −80 mV to voltages between −30 and +50 mV in 10-mV steps. Tail currents at −50 mV. Horizontal bar above top tracing indicates 250 ms (duration of steps as in Fig. 3). (*B*) Voltage dependence of inactivation. Peak current was measured at +50 mV (see inset) after 5-s conditioning prepulses to voltages between −100 and +20 mV. Full inactivation was not achieved in 5 s (see *A*). Calibration for inset: 25 ms, 1 nA. (*C*) The current during the depolarizing step to +40 mV (*A*) is displayed in semilogarithmic format. The two components of the double exponential fit are shown. The slow component is superimposed on the original data points; the fast component was superimposed on data points calculated by subtracting the slow component. The residuals of the fit, i.e., the deviation of the data points from the fitted curve, are shown in the top section. The residuals for the double exponential fit (shown in the main panel) are labeled *2 exp*. For comparison, the residuals of the monoexponential fit (*1 exp*) are also shown. The latter showed nonrandom runs of positive and negative deviations, which were eliminated in the double exponential fit. A single exponential was therefore not sufficient to describe the time course of slow inactivation. (*D*, *E*) Voltage dependence of kinetics of slow inactivation, and the relative amplitude of the fast component (average 46 ± 3% of total inactivating current). Data from five to eight experiments (mean ± SD).

Effect of Temperature

Fig. 9 shows a superposition of HK2 currents obtained at +50 mV under standard conditions (room temperature) and after cooling to 17°C (Fig. 9 *A*) or warming to 34°C (Fig. 9 *B*). Reduction of temperature resulted in a slower activation time course. At the higher temperature a larger peak current level was attained, and channel activation proceeded faster with a time constant of 350 μs (compared with 1.8 ms at 24°C in this cell). This faster and enhanced activation was followed by a more extensive inactivation. Qualitatively similar results were obtained in four other cells.

Effects of 4-AP, La^{3+}, Dendrotoxin, Clofilium, and TEA

Several mammalian *Shaker*-derived K^+ channels differ in their sensitivity to classical K^+ channel blockers such as 4-AP and TEA, and neurotoxins such as DTX-I. For comparison with other mammalian K^+ channels, the sensitivity of HK2 to these agents was determined. The reduction of HK2 current by 4-AP (500 μM) is illustrated in Fig. 10 *A*. Using the suppression of current at the end of a 250-ms depolarization to +50 mV as an index of block, a concentration–response curve was obtained with an apparent affinity (IC_{50}) of 180 μM (Fig. 10 *B*). In contrast to this high sensitivity

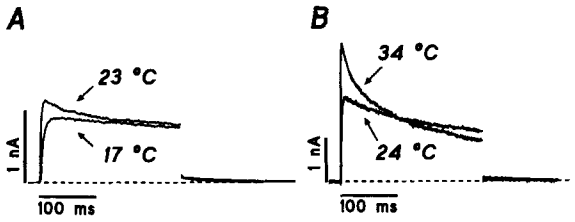

FIGURE 9. Temperature dependence of HK2 kinetics. Superimposed tracings for depolarization from −80 to +50 mV at different temperatures. (*A*) Decrease from 22 to 15°C. (*B*) Increase from 24 to 34°C. Results are from different experiments.

for 4-AP, the HK2 current was not very sensitive to TEA: the reduction was <20% (n = 3) for either the peak current or 250 ms current with 10 mM external TEA (Fig. 10 *E*).

To help in the discrimination between Kv1.2 and Kv1.5 as cloned channels potentially corresponding to a rapidly activating cardiac K^+ channel, the sensitivity of HK2 to DTX-I was determined. HK2 was essentially unaffected by a high concentration of DTX-I: the reduction of current was 3 ± 2% (n = 3) with 100 nM DTX-I.

In cardiac myocytes, 10 μM La^{3+} completely blocks the "rapid" component (I_{Kr}) of delayed outward K^+ current (Balser et al., 1990; Sanguinetti and Jurkiewicz, 1990*a*, *b*). Fig. 10 *C* shows that a 20-fold higher concentration (200 μM La^{3+}) reduced the HK2 current by only 13%. Nevertheless, La^{3+} had a marked effect on the voltage dependence of HK2 activation. Fig. 10 *D* shows that the activation curve was shifted by 23 mV in the depolarizing direction, with a concomitant slowing of the activation kinetics. Similar results were obtained in three experiments.

Fig. 10 *F* shows that 1 μM clofilium reduced the HK2 current during depolarization in a time-dependent manner to 35% of control at the end of the step. Similar results were obtained for this concentration in four experiments.

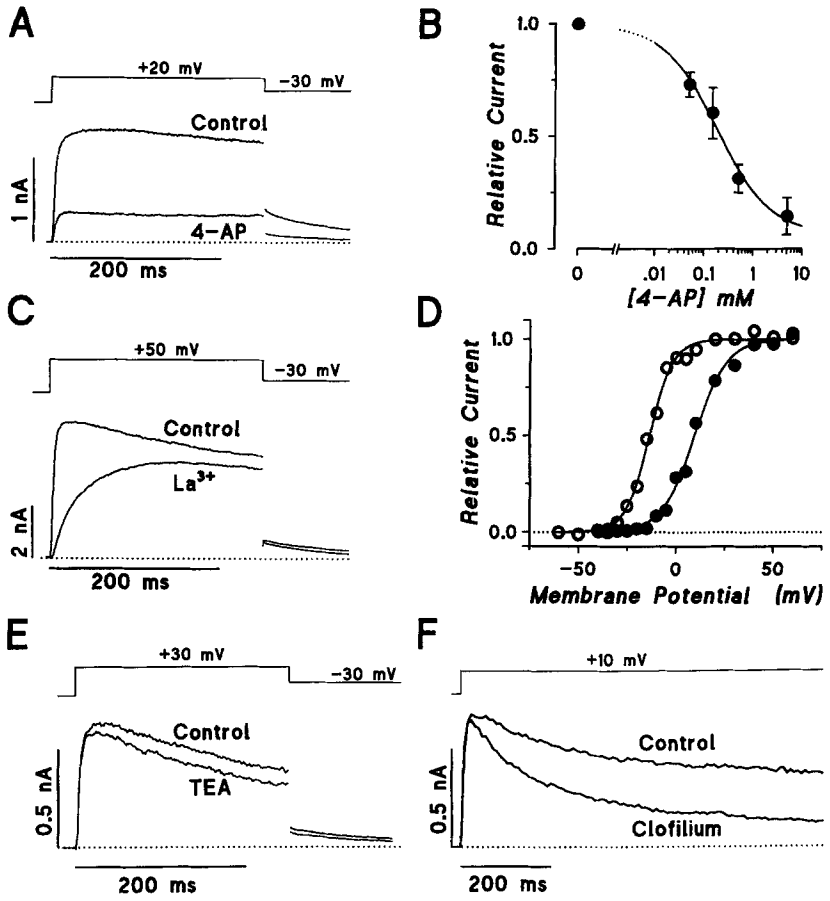

FIGURE 10. Effects of 4-AP, TEA, La^{3+}, and clofilium on HK2. (*A*) Effect of 4-AP on HK2 current. The current (obtained at +20 mV) was reduced by 75% compared with control after application of 500 μM 4-AP. (*B*) Concentration–response curve. The relative reduction of the 250-ms current at +50 mV was used as an index of block. Pooled data from 10 experiments. The solid line is drawn according to the Hill equation $y = 1/(1 + K_D/[4\text{-AP}])^n$ fitted to the data with the following parameters: apparent affinity IC_{50} = 181 μM and Hill coefficient n = 0.85. (*C*) Modification of HK2 current by La^{3+}. Tracings for this pulse protocol (*top*) are shown for control and after 200 μM La^{3+}. The current at the end of the step was reduced by 13%. Electrode resistance was 1.25 MΩ, and residual access resistance (see Methods) was estimated at 0.7 MΩ. (*D*) Voltage dependence of channel opening. Data were obtained from tail currents at −30 mV as in Fig. 7 *A*. *Open circles*, control; *filled circles*, 200 μM La^{3+}. Solid lines are drawn using the Boltzmann equation with respective midpoints of −14 and +9 mV. The amplitude in La^{3+} was 85% of control. (*E*) Effect of extracellular application of 10 mM TEA. Current was reduced by only 16% at the end of the 250-ms step. (*F*) Effect of 1 μM clofilium. Reduction of HK2 current by 65% at the end of a 1-s depolarization after a 30-min equilibration with clofilium. Note the compressed time scale.

DISCUSSION

Under the experimental conditions used in this study, voltage-gated K^+ currents were only observed in the HK2-transfected mouse L cells. This tissue culture system has potential advantages over the commonly used oocyte expression system. The clonal cell line has been stable for over two years with highly reproducible results: this may alleviate problems associated with variability in oocyte quality. The mammalian cells may also process the channel protein more similar to the native cells: glycosylation may, for instance, be incomplete in oocytes (Sutton, Davidson, and Lester, 1987; Thornhill and Levinson, 1987; Pfaff, Tamkun, and Taylor, 1990), and anomalous gating behavior has been reported for μI Na^+ channels expressed in oocytes but not in mammalian cells (Ukomadu, Zhou, Sigworth, and Agnew, 1992). Using clonal cell lines with adequate expression levels, channel protein isolation and purification will be more practical and more easily achieved.

Compared with native myocytes, this model system offers improved voltage clamp quality and speed due to small cell size. In addition, the absence of other contaminating K^+ and non-K^+ currents eliminates the need for various ionic substitution or subtraction techniques. We will now discuss in more detail the expression system and the channel properties compared with other *Shaker*-like channels and with currents in native myocytes. Where possible, we will also discuss properties in relation to the primary structure.

Stable Expression

This is the first detailed characterization of a K^+ channel cloned from human heart and expressed in mammalian cell lines. In the HK2 transfected cell lines, a current with delayed rectifier properties was observed that was absent in nontransfected and sham transfected cells. Other L cell lines transfected with different K^+ channels from the rat cardiovascular system displayed clone-specific phenotypes in the same expression system (Snyders, Fish, Roberds, Knoth, Tamkun, and Bennett, 1991*b*). In addition, the rat K^+ channel Kv1.1 cloned from rat aorta as RK1 (Roberds and Tamkun, 1991*a*), which is identical to RCK1 cloned from rat brain (Stühmer et al., 1988) has now been expressed in three different mammalian cell lines with identical phenotype: Sol-8 cells (Koren et al., 1990), L cells (Snyders et al., 1991*b*), and CHO cells (Snyders, D. J., S. L. Roberds, K. M. Deal, and M. M. Tamkun, unpublished observations).

It has been suggested that continuous overexpression of exogenous K^+ channels might pose a growth disadvantage for transfected cells (Koren et al., 1990). In our hands, a cell line expressing a rat cardiovascular channel (RK2, Kv1.2) driven by a constitutively active CMV promoter yielded over time fewer cells expressing this current (Snyders, D. J., S. L. Roberds, K. M. Deal, and M. M. Tamkun, unpublished observations). Therefore, we used a dexamethasone inducible promoter in the transfection construct (Fig. 1 *A*) to establish the HK2 cell line. In addition, the same vector included the neomycin resistance gene and therefore it would be expected that a cell that lost the HK2 gene would also lose neomycin resistance and not survive under the culture conditions. The stable expression for over two years demonstrates

the success of this approach and indicates that the hardly detectable expression (if any) without induction did not pose a problem for this cell line.

Lack of Contaminating Currents

Although no attempt was made to eliminate Na^+ and Ca^{2+} currents, none were observed in either sham or HK2 transfected cells ($n > 300$). The lack of detectable Ca^{2+} current is consistent with the lack of endogenous dihydropyridine receptors or Ca^{2+} current in a similar mouse L cell line (Perez-Reyes, Kim, Lacerda, Horne, Wei, Rampe, Campbell, Brown, and Birnbaumer, 1989; Varadi, Lory, Schultz, Varadi, and Schwartz, 1991).

In other L cell lines, Ca^{2+}-activated K^+ channels have been observed, or at least implicated indirectly to explain hyperpolarizing responses to various stimuli (Hosoi and Slayman, 1985; Okada, Yada, Ohno-Shosaku, and Oiki, 1986). We failed to identify any such currents, if present in our cell line, possibly due to the intracellular buffering with BAPTA (which was chosen for its faster Ca^{2+} binding rate compared with EGTA). In some mouse L cell lines, a nonselective cation channel with a conductance of 25–30 pS has been reported (Frace and Gargus, 1985), which was activated by platelet-derived growth factor. We have observed a similar channel in cell-attached patches and it is possible that this channel contributed to the time-independent leak current observed in the whole cell recordings.

It may be difficult to compare the various cell lines because the L cell strains kept in different laboratories are not identical. However, the main point here is that although some other ion channels may exist in this cell line, they did not generate currents (under the experimental conditions used) that contaminated or complicated the analysis of selectivity, rectification, and gating of the expressed human cardiac K^+ channel. In addition, the envelope of tails test (Hodgkin and Huxley, 1952) was satisfied, indicating expression of a homogenous population of channels.

HK2 Is a Highly Selective K^+ Channel

The HK2 clone was obtained from a human ventricular cDNA library and displayed homology with *Shaker* K^+ channels. The K^+ selectivity of the HK2 channel was confirmed by the dependence of its reversal potential on the external K^+ concentration (Fig. 5). The slope of 55 mV/decade compares well with the values generally obtained for other K^+ channels of the *Shaker* family, and is close to the theoretically expected value of 59 mV/decade calculated from the Nernst equation. Based on the 32-mV change in reversal potential between 4 and 16 mM external K^+, and assuming that only monovalent cations would permeate through the channel, a selectivity ratio $\alpha = P_{Na}/P_K$ of 0.007 can be obtained from $\Delta E = RT/F \times \ln [(\alpha Na_{o1} + K_{o1})/(\alpha Na_{o2} + K_{o2})]$, with $\Delta E = -32$ mV, $Na_{o1} = 145$, $K_{o1} = 4$, $Na_{o2} = 133$, and $K_{o2} = 16$. The same result was obtained by fitting the GHK voltage equation (Goldman, 1943; Hodgkin and Katz, 1949) to the data in Fig. 5: $P_{Na}/P_K = 0.007 \pm 0.001$.

Rectification

A second important feature of this channel is its outward rectification. This is clearly illustrated by the fully activated current–voltage relationship in Fig. 6, *A* and *B*. The

rectification is also evident in the smaller than expected tail current amplitudes at −30 and −50 mV. For example, in Fig. 3 the current at +50 mV was 1,320 pA, while the tail current at −30 mV was only 205 pA, a ratio of 0.16. For a linear current–voltage relationship a value of 0.38 would be expected (using a reversal potential of −80 mV). This smaller than expected ratio was observed in all envelope of tails experiments, in which the ratio was measured for different combinations of step and tail potentials (Table II). For the results shown in Fig. 4, the observed ratios were 0.36 and 0.24, compared with 0.62 and 0.50 expected in the absence of rectification.

The curves superimposed on the data in Fig. 6, *A* and *B* were calculated from the GHK constant field equation (Goldman, 1943; Hodgkin and Katz, 1949). The degree of rectification in this model is determined by the K^+ concentrations (more correctly, ion activities) on either side of the membrane, scaled by P_K (the only free parameter). The curves in Fig. 6, *A* and *B* were well described by this GHK equation. The values of P_K obtained from fitting the equation to the data points in 4 mM $[K]_o$ and 16 mM

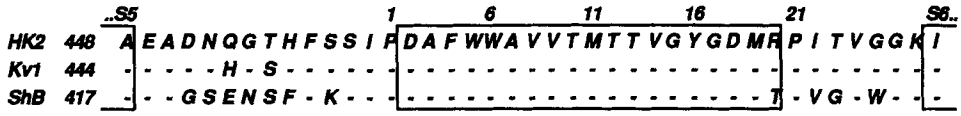

FIGURE 11. K channel pore region. Comparison of the amino acid sequence of HK2, Kv1, and *Shaker B* (*ShB*) between the putative transmembrane-spanning domains S5 and S6 (open-ended box at either end). Amino acids are shown in one-letter code. Dashes indicate amino acids conserved between HK2 and Kv1 or ShB, respectively. 417, 448, and 444 refer to the positions in the respective channel sequences of the first amino acid shown, which were used for sequence alignment. The central box indicates the core of the ion conducting pore, numbered according to Durell and Guy (1992). The only difference between pore sequence of ShB and of HK2 and Kv1 is at pore position 20: the neutral amino acid (*T*, threonine) in ShB is replaced by a positively charged residue (*R*, arginine) in HK2 and Kv1.

$[K]_o$ were similar, but the value for 75 mM was smaller. Thus, the constant field prediction holds well for the 4 and 16 mM $[K]_o$ data, but predicts more outward current for 75 mM than experimentally observed. The latter suggests that the GHK model may not fully explain the rectification behavior, and that other factors such as ion–ion interactions or other models—for instance, based on rate theory—may be required (Eyring, Lumry, and Woodbury, 1949; Hille, 1991).

It is known that several K^+ channels of the *Shaker* family display inward rectification with symmetrical transmembrane K^+ concentrations (Koren et al., 1990; MacKinnon and Yellen, 1990; Yool and Schwarz, 1991). This characteristic appears to depend on the charge of the residue at the T449 equivalent position: when the threonine at this site was mutated to a positively charged arginine or lysine, inward rectification was absent (MacKinnon and Yellen, 1990); HK2 has an arginine at this position (Fig. 11; Tamkun et al., 1991). Therefore, the approximately linear current–voltage relationship of HK2 in high external K^+ is consistent with the rectification properties observed for *Shaker* channels and their mutants. Molecular

modeling of the pore has suggested that this residue is located at the external end of the narrow section of the pore (Durell and Guy, 1992).

At lower K^+ concentrations, a GHK formalism described the rectification of the current–voltage relationship reasonably well. As the cell dialysis presumably prevented significant changes in internal K^+ concentration, the pronounced rectification effect should result from the external K^+ ion concentration. This reduction of inward current, especially at low external K^+ concentration, could thus be due to the concentrated positive charge resulting from the putative ring of four arginine residues at the external mouth of the HK2 channel (Durell and Guy, 1992). In support of this, the loss of rectification in *Shaker* mutations at this site was due to a reduced inward conductance (MacKinnon and Yellen, 1990). Similar effects of concentrated positive and negative charges at either end of the pore have been observed for the rectification properties of the muscle acetylcholine receptor channel (Imoto, Busch, Sakmann, Mishina, Konno, Nakai, Bujo, Mori, Fukuda, and Numa, 1988). Site-directed mutagenesis of this cloned cardiac K^+ channel will allow the hypothesis that these charged residues are responsible for the observed rectification to be tested, which may help to elucidate the molecular basis for rectification in cardiac ion channels in general.

Channel Activation Kinetics

The lack of overlapping currents in this system clearly revealed that the time course of HK2 channel opening was sigmoidal (Fig. 7 *B*). This delayed activation requires multiple nonconducting states before the open state. Based on the probable four-subunit composition of this channel (MacKinnon, 1991; Liman, Tytgat, and Hess, 1992), activation kinetics were fitted using an $n = 4$ formalism (Hodgkin and Huxley, 1952). In many cells this resulted in a reasonable fit of the activating current. However, this result cannot be taken as firm evidence to propose that channel opening results from the independent gating of four subunits. At low depolarizations, tracings were better fit with a lower power, and when tracings were well fit with $n = 4$, it was difficult to differentiate statistically among $n = 3$, 4, or 5. In addition, at strong depolarizations, an n^4 model usually resulted in an insufficient initial delay, in which case a better fit for the initial delay would have required a much higher power, as observed, for instance, for the DRK1 (Kv2.1) channel (VanDongen, Frech, Drewe, Joho, and Brown, 1990). Furthermore, the implicit assumption that activation of the four subunits proceeds independently is probably an oversimplification. Although the present results cannot discriminate reliably between the exact number of activation subunits, and whether each activates independently, the sigmoidicity of the activation time course does require a transition through multiple nonconducting states, and is consistent with a four-subunit activation scheme, including a permissive state from which opening occurs in a voltage-independent manner, as proposed for other channels of the *Shaker* family (Koren et al., 1990; Zagotta and Aldrich, 1990).

Voltage Dependence of Channel Opening

The voltage dependence of opening of this channel occurs at fairly positive potentials. This is similar to the voltage dependence of activation of an insulinoma K^+ channel hPCN1 (Philipson, Hice, Schaeffer, LaMendola, Bell, Nelson, and Steiner, 1991). This channel displayed 98% homology with HK2, and activated at ~ 8

mV more positive potentials when expressed in *Xenopus* oocytes. It is unclear whether this small difference is significant. In addition, the activation time courses for HK2 and hPCN1 were similar. For hPCN1, the activation time constants were obtained from monoexponential fits (Philipson et al., 1991) and the resulting values were similar to those obtained for HK2 using the same method (Fig. 7 *C*, Table III).

The slope factor of the activation curve k = 5.9 mV obtained in this study is somewhat steeper that the value obtained for hPCN1 in oocytes (k = 6.9 mV; Philipson et al., 1991), but both are much steeper than the value (k = 15 mV) obtained for the rat homologue brain channel Kv1 (Swanson, Marshall, Smith, Williams, Boyle, Folander, Luneau, Antanavage, Oliva, Buhrow et al., 1990). This could be due to the lower degree of homology between HK2 and Kv1 (86%); however, the number of charges in the S4 domain (putative voltage sensor) are identical. Therefore, the difference may be due to the different methods used to obtain the activation curve. For Kv1 the value refers to the voltage dependence of

TABLE III

Comparison of Cardiac Delayed Rectifier and Cloned K⁺ Channels

	I_{Ks}	I_{Kr}	I_{Kp}	I_{Kd}	HK2	hPCN1	Kv1
V_h	+20	−9	~−20	−2*	−14	−6	~0*
k	15	22	Shallow	14*	6	6.7	17*
τ(0/+60)	5,000/1,000	50/15	5 (+80 mV)	5/1.4‡ (0/+50 mV)	5/1.5‡ 10/1.8§	8.3/1.4§	NR
Inactivation	No (5,000 ms)	No (225 ms)	No (500 ms)	Partial	Partial	Partial	NR
Rectification	Linear	Inward	Linear?	Outward	Outward	NR	NR

NR, not reported. Activation curves: V_h, midpoint (millivolts); k, slope factor (millivolts).
*Activation curve obtained from G/G_{max}. τ, time constant (ms) for activation at 0 and +60 mV.
‡HH fit, n = 4.
§Exponential fit.

normalized conductance (G/G_{max}), an analysis in which the conductance at each voltage was obtained by dividing current by driving force assuming a linear current–voltage relationship. If the Kv1 channel displays outward rectification similar to HK2, then this method of estimating the voltage dependence would result in an underestimation of the slope factor as illustrated by the dotted line in Fig. 7 *A* (see also VanDongen et al., 1990; Hille, 1991) and explain the difference in the numerical values. Of interest in this regard is the Kv1 pore sequence that is identical to HK2, including the arginine at the *Shaker* T449 equivalent site (Fig. 11).

Comparison of the Slow Inactivation to Inactivation Mechanisms of Other Shaker-related K⁺ Channels

We consider the slow inactivation of HK2 (Fig. 8) to be a genuine gating property and not an artifact from K^+ accumulation, because it (*a*) was independent of the size of the current, (*b*) was present in 140 mM $[K^+]_o$, and (*c*) was steeply voltage dependent in a voltage range where minimal K^+ current is activated (−30 to −20 mV).

This slow inactivation observed for HK2 appears to be a property shared by other K^+ channels of the *Shaker* family (Iverson and Rudy, 1990; Hoshi, Zagotta, and

Aldrich, 1991). In *ShB,* two modes of inactivation can be distinguished: N-type and C-type (Choi, Aldrich, and Yellen, 1991; Hoshi et al., 1991). The N-type inactivation appears to occur by a "ball-and-chain" mechanism (Hoshi, Zagotta, and Aldrich, 1990), in which the intracellular NH_2-terminal end of the channel blocks the ion-conducting pore. Most evidence indicates that inactivation by this mechanism requires prior channel opening (Bezanilla, Perozo, Papazian, and Stefani, 1991; Demo and Yellen, 1991; Ruppersberg, Frank, Pongs, and Stocker, 1991), and that the putative receptor for this inactivating "ball" is part of the intracellular mouth of the ion-conducting pathway (Isacoff, Jan, and Jan, 1991). This mode of inactivation is generally fast. The second mode of inactivation, C-type inactivation, appears to involve the last membrane-spanning helix S6 (Hoshi et al., 1991); i.e., the transmembrane domain closest to the COOH-terminal end of the channel. This mode of inactivation was initially considered to occur only on a slow time scale, but more recent data indicate that *ShB* can be mutated to inactivate rapidly by this mechanism. The amino acid at position 463 in *ShB* has been shown to influence the rate of inactivation. An alanine at this position results in inactivation time constants of ~ 3 s, while with a valine at this position, much faster time constants of <30 ms are obtained (Hoshi et al., 1991). In *ShB* the (slow) time constant for C-type inactivation is virtually independent of membrane potential (Hoshi et al., 1991). Based on the functional results obtained for HK2 (Fig. 8) and on sequence homology, we infer that the inactivation mechanism of HK2 is probably C-type because (*a*) the kinetics of slow inactivation of HK2 were almost voltage independent, (*b*) HK2 has an alanine at the equivalent position in the S6 domain, and (*c*) HK2 does not have a long NH_2-terminal domain with homology to the N-type inactivation ball (Tamkun et al., 1991).

The steep voltage dependence of this inactivation process contrasts sharply with the near voltage independence of the time constants. The latter suggests that the slow inactivation process derives its voltage dependence not from voltage-sensitive rate constants, but from the voltage dependence of channel opening or activation (Hoshi et al., 1990, 1991). In our experiments, (*a*) the voltage dependence of inactivation overlapped with the lower part of the curve describing the voltage dependence of channel opening, (*b*) the difference between activation and inactivation midpoints was ~ 8 mV, and (*c*) inactivation could be detected in a test pulse only if some degree of channel opening could be detected during the preceding pulse. With a more negative midpoint, the latter would result in an inactivation curve with steeper voltage dependence compared with that of activation (Zagotta and Aldrich, 1990). In fact, it has been proposed that under these conditions the slope factor of passive voltage dependence of inactivation may be a reasonable estimator of the gating charge involved in channel activation (Zagotta and Aldrich, 1990). The slope factor of 3.7 would in this case suggest a gating charge of at least 6.9 elementary charges for HK2 activation.

In the insulinoma channel hPCN1 (Philipson et al., 1991), slow inactivation has also been observed. The voltage dependence of inactivation of hPCN1 (midpoint -25 mV, slope factor 3.8 mV) was similar to that of HK2 and overlapped with the voltage dependence of activation, as was observed for HK2. The kinetics of slow inactivation showed only weak voltage dependence. However, contrary to HK2, only a single time constant for inactivation was described. This difference could be due to the small differences in the channel sequence (2%) or to the different heterologous

expression systems (oocytes for hPCN1, mammalian cells for HK2), as has been observed for Na^+ channel inactivation kinetics in amphibian and mammalian expression systems (Ukomadu et al., 1992). However, a monoexponential fit of a biexponential process with time constants as in Fig. 8 could also result in an intermediate time constant of ~1 s. The distinction between the number of kinetic components in the slow inactivation is important, because the observation of two time constants in the inactivation process indicates the presence of at least two inactivated states (either in parallel or consecutive). In other experiments where 30–45 second depolarizations were used, an additional very slow component was observed with time constants >10 s).

Comparison of the Expressed Current to Currents Recorded in Native Myocytes

Table III compares several properties of delayed rectifiers in cardiac myocytes with the characteristics of HK2. The main properties of HK2 are activation at fairly positive potentials (plateau range of cardiac action potential), fast activation kinetics, slow inactivation, and outward rectification dependent on external K^+ concentration. Based on these properties, we will discuss the K^+ currents identified in native cardiac myocytes to which the HK2 current may correspond.

The delayed outward rectifier current in guinea pig myocytes is composed of at least two components (Balser et al., 1990; Sanguinetti and Jurkiewicz, 1990*a*): a slowly activating component (I_{Ks}) and a rapidly activating one (I_{Kr}). It does not appear that the HK2 current corresponds to either of these currents. I_{Ks} activates at more positive voltages with a time course that is about three orders of magnitude slower than HK2 activation (Matsuura, Ehara, and Imoto, 1987; Balser et al., 1990; Sanguinetti and Jurkiewicz, 1990*a*). I_{Ks} does not inactivate during 5–10-s depolarizations, and its rectification is either linear or slightly inward. In addition, heterologous expression of a different cloned K^+ channel (I_{sK}) resulted in a current with characteristics that correspond reasonably well to those of I_{Ks} (Takumi, Ohkubo, and Nakanishi, 1988; Murai, Kakizuka, Takumi, Ohkubo, and Nakanishi, 1989; Folander, Smith, Antanavage, Bennett, Stein, and Swanson, 1990). The rapid component I_{Kr} activates in the same voltage range as HK2, but has several features that are quite different from the HK2 current. First, although designated rapid, the activation time course of this current component is about an order of magnitude slower than that of HK2. Second, I_{Kr} displays marked inward rectification: at +50 mV, the maximum current is only 30% of that at 0 mV (Sanguinetti and Jurkiewicz, 1990*a*). Third, the I_{Kr} current is fully suppressed by 10 μM La^{3+} (Sanguinetti and Jurkiewicz, 1990*b*), whereas HK2 is hardly affected at 200 μM. Whether this current inactivates during longer depolarizations is unclear at present, but the observed differences make it unlikely that the HK2 clone corresponds to this current in native myocytes. In guinea pig myocytes another K^+ current, designated I_{Kp}, has been described (Yue and Marban, 1988). This I_{Kp} current did not inactivate during a 500-ms depolarization to +80 mV, and compared with HK2 appeared to activate with a more shallow voltage dependence and at more negative potentials (Yue and Marban, 1988). In addition, the 14-pS conductance of I_{Kp} was insensitive to changes in external K^+ concentration between 1 and 7 mM, and declined slightly at higher concentrations. No outward rectification was reported for this current. These differences make it unlikely that the HK2 current corresponds to the I_{Kp} current.

K^+ currents with delayed outward rectifier properties and fast activation kinetics at room temperature have recently been described in rat atrial myocytes (Boyle and Nerbonne, 1991) and neonatal canine epicardial ventricular myocytes (Jeck and Boyden, 1992). These currents could be abbreviated I_{Kd} (depolarization). In both cases, the voltage range of activation, activation kinetics, and rectification properties correspond well to those observed for HK2 (Table III). In addition, both rat and canine I_{Kd} display slow inactivation during 250-ms depolarizations, which is more complete during longer depolarization (Boyle and Nerbonne, 1992; Jeck and Boyden, 1992). In addition, this I_{Kd} channel in rat atrial myocytes displayed a biexponential time course of slow inactivation. While this might be due to two functionally different currents (Boyle and Nerbonne, 1992), the results compare very closely to our observations regarding the slow inactivation of HK2 (human Kv1.5). An important point in this comparison is that a closely related channel cloned from rat heart (RK4, rat Kv1.5) is expressed more abundantly in rat heart than in other tissue and is the first K^+ channel detected during early embryonic cardiogenesis, whereas all other rat cardiac K^+ channels cloned to date only appear later during development (Roberds and Tamkun, 1991*b*).

Comparison with K^+ Currents in Human Atrium

Northern analysis has shown that HK2 mRNA is expressed in human atrium to a greater extent than in human ventricle (Tamkun et al., 1991). Therefore, it is of interest to compare the properties of the HK2 current with those of human atrial K^+ currents. In human atrial myocytes, several K^+ currents have been described: an inward rectifier I_{K1}, ligand-gated currents $I_{K(ATP)}$ and $I_{K(ACh)}$, and two components of transient outward current I_{TO} or I_A (Escande, Coulombe, Faivre, Deroubaix, and Coraboeuf, 1987; Shibata, Drury, Refsum, Aldrette, and Giles, 1989; Heidbüchel, Vereecke, and Carmeliet, 1990). The question here is whether HK2 represents a yet unrecognized current, or whether it represents a voltage-gated component of I_A in these cells.

At room temperature the time course of inactivation of HK2 is much slower than that of the transient outward currents reported in human atrium (Escande et al., 1987; Shibata et al., 1989). In both studies recording conditions were used under which calcium-activated components were absent or minimized, similar to the whole cell recording conditions reported in this paper. Under these conditions, the human atrial I_A did not fully inactivate. Fig. 5 *C* of Escande et al. (1987) and Fig. 2 *A* of Shibata et al. (1989) reveal a noninactivating component (20–40% of total outward current at +40 mV) with fast activation kinetics. The sustained component was at least as sensitive to 500 μM 4-AP as the larger inactivating K^+ current (Fig. 4 *B* in of Shibata et al., 1989). It is not clear whether this sustained component is noninactivating I_A or represents a separate current. Important here is that HK2 is indeed very sensitive to 4-AP (75% suppression by 500 μM 4-AP). It is therefore possible that HK2 corresponds to a noninactivating current component in these human atrial cells. In addition, the high sensitivity to 4-AP and the more pronounced I_A-like behavior of HK2 at higher temperatures raise the question of whether this cloned channel could contribute to currents that might be identified as I_A current at physiological temperature.

Pharmacological Properties

The HK2 current is blocked by quinidine at clinically relevant concentrations (Snyders et al., 1992*a*). Quinidine appeared to block preferentially the open state in a voltage-dependent manner consistent with an intramembrane binding site 19% from the intracellular face of the membrane. This suggested that a quaternary ammonium binding site may be involved (Armstrong, 1971). The results with the quaternary ammonium antiarrhythmic agent clofilium (Snyders et al., 1992*b*) support this idea and suggest a high affinity of HK2 for clofilium (Fig. 10 *F*). The latter may be significant because clinically used concentrations of clofilium are much lower than those needed to block I_{Ks} (Snyders and Katzung, 1985; Arena and Kass, 1988) or its putative clone I_{sK} (Folander et al., 1990). Therefore, the HK2 current may represent the clofilium-sensitive current in human heart.

The low sensitivity to external TEA is consistent with the results of mutations of the external mouth of the pore of various K^+ channels of the *Shaker* family. With a positively charged amino acid at pore position 20 (Fig. 11, corresponding to 480 in HK2 476 in Kv1 and 449 in *Shaker B*), a low affinity has been observed in all native or mutated channels (MacKinnon and Yellen, 1990; Kavanaugh, Varnum, Osborne, Christie, Busch, Adelman, and North, 1991). Similar results have been reported for the rat homologue Kv1, which also has a low affinity ($IC_{50} > 100$ mM) and in which the mutation of the arginine at position 476 (Fig. 11) into tyrosine (R476Y) introduced high affinity for external TEA ($IC_{50} = 0.4$ mM; Liman, Tytgat, and Hess, 1992). The low TEA sensitivity of HK2 is also consistent with the lack of effect of external TEA on K^+ current and action potential duration in cardiac preparations (Kass, Scheuer, and Malloy, 1982; Gintant et al., 1991).

In contrast, the sensitivity of this channel to 4-AP is surprisingly high. The >75% suppression by 500 μM 4-AP observed for HK2 is similar to that reported for closely related channels (hPCN1, Kv1), and the small differences probably relate to different pulse protocols used to determine the degree of block. Indeed, the complicated time, voltage, and rate dependency of 4-AP block has long been recognized (Yeh, Oxford, Wu, and Narahashi, 1976), and in preliminary experiments we have observed a strong dependency of 4-AP block on membrane potential, resulting in >95% block with 500 μM 4-AP when holding at −30 mV. The sensitivity of HK2 to 4-AP further supports the possibility that HK2 corresponds to the native I_{Kd} current in rat atrial myocytes (Boyle and Nerbonne, 1991). However, a similar current reported in neonatal dogs (Jeck and Boyden, 1992) appeared much less sensitive to 4-AP. In cardiac Purkinje fibers, suppression of both a transient outward (Kenyon and Gibbons, 1978) and a sustained plateau current (Van Bogaert and Snyders, 1982) have been described with 4-AP concentrations as low as 100 μM.

The HK2 channel was found to be insensitive to nanomolar concentrations of DTX-I. This is in agreement with results obtained for the homologous channel Kv1, which was unaffected by 200 nM DTX-I (Swanson et al., 1990). In related mammalian K^+ channels it has also been shown that a negatively charged amino acid at position 454 is an important determinant for high affinity DTX-I binding (Hurst et al., 1991). Both HK2 and Kv1 have an identical uncharged residue at this position (G454; Fig. 11). Although the sensitivity of K^+ currents in native cardiac myocytes has not yet

been reported, the differential DTX-I sensitivity between the RK2 clone (IC_{50} = 0.4 nM; Hurst et al., 1991) and HK2 (IC_{50} > 100 nM) should be useful in ruling out at least one of these clones as corresponding to the fast activating current in rat atrial myocytes.

The effects of 200 μM La^{3+} we observed were largely a reflection of a shift in the voltage dependence of activation and activation kinetics and may, in addition, involve some degree of block at negative potentials similar to effects seen in cardiac cells (Sanguinetti and Jurkiewicz, 1990*b*). Shifts such as these are frequently observed with divalent and trivalent cations (Hille, 1991). However, further analysis of the trivalent cation effects was beyond the scope of this paper.

Electrophysiological and pharmacological correspondence alone are probably insufficient to formally identify a cloned K^+ channel with any K^+ current present in native cells. Small differences in kinetics may be due to some different modulation of the channel in each expression system. Formal identification will require in situ hybridization and immunohistological localization, and preferably immunoelectrophysiological correspondence—a specific monoclonal antibody producing a similar functional effect in a channel in native cells and the corresponding putative cloned channel—in addition to functional and pharmacological correspondence. At present, no cloned K^+ channel has formally been identified with a K^+ channel in native cardiac cells in this way, and it is not known whether the native channels are pure homotetramers or consist of different subunits.

Possible Function of HK2

As pointed out earlier, a definite correspondence between this channel clone and a K^+ current in native myocytes remains to be established. However, the functional properties suggest that this current can be involved both in early repolarization and in control of plateau duration. It is important to note that the transient outward currents produce the early fast repolarization, not because of their transient nature, but because of their fast activation kinetics. This property is shared by the cloned HK2 and native I_{Kd} currents (Boyle and Nerbonne, 1991; Jeck and Boyden, 1992), and therefore these currents can easily contribute to a fast repolarization to the plateau range of potentials. However, a large sustained outward current could repolarize the cardiac action potential prematurely. The inactivation of I_A currents, the outward rectification of the I_{Kd} and HK2 currents, and the level of expression provide three mechanisms that would prevent these currents from fully repolarizing the action potential, especially with the concomitant activation of the calcium current. Therefore, it seems reasonable to expect a modulatory effect of the HK2 current on action potential duration, as has been suggested for the very similar native current I_{Kd} (Boyle and Nerbonne, 1991). In addition, the sensitivity of the HK2 current to quinidine and clofilium would suggest that HK2 is a target for class III antiarrhythmic agents. In this respect the stable mammalian cell culture expression provides a powerful system for drug development and for elucidating structure–function analysis of drug–channel interactions.

We thank Dr. James Johns for review of the manuscript and for the use of his 486 computer on which most of the analysis was done, Dr. Dan Roden for critical review of the manuscript, and Mr. Craig Short for technical assistance.

Supported by NIH grants RR-05424 and HL-47599 (to D. J. Snyders), HL-40608 (to P. B. Bennett), GM-41325 (to M. M. Tamkun), and HL-46681 (to D. J. Snyders, P. B. Bennett, and M. M. Tamkun), a Grant-in-Aid from the American Heart Association and Winthrop Pharmaceuticals (to M. M. Tamkun), and the Stahlman Endowment (to D. J. Snyders). M. M. Tamkun and P. B. Bennett are Established Investigators of The American Heart Association.

Original version received 18 May 1992 and accepted version received 10 December 1992.

REFERENCES

Agus, Z. S., I. A. Dukes, and M. Morad. 1991. Divalent cations modulate the transient outward currents in rat ventricular myocytes. *American Journal of Physiology.* 261:C310–318.

Arena, J. P., and R. S. Kass. 1988. Block of heart potassium channels by clofilium and its tertiary analogs: relationship between drug structure and type of channel blocked. *Molecular Pharmacology.* 34:60–66.

Armstrong, C. M. 1976. Interaction of tetraethylammonium ion derivatives with the potassium channels of giant axons. *The Journal of General Physiology.* 58:413–437.

Balser, J. R., P. B. Bennett, and D. M. Roden. 1990. Time dependent outward current in guinea pig ventricular myocytes. Gating kinetics of the delayed rectifier. *The Journal of General Physiology.* 96:835–863.

Benishin, C. G., R. G. Sorensen, W. E. Brown, B. K. Krueger, and M. P. Blaustein. 1988. Four polypeptide components of green mamba venom selectively block certain potassium channels in rat brain synaptosome. *Molecular Pharmacology.* 34:152–159.

Bezanilla, F., E. Perozo, D. M. Papazian, and E. Stefani. 1991. Molecular basis of gating charge immobilization in Shaker potassium channels. *Science.* 254:679–683.

Boyle, W. A., and J. M. Nerbonne. 1991. A novel type of depolarization-activated K^+ current in adult rat atrial myocytes. *American Journal of Physiology.* 260:H1236–H1247.

Boyle, W. A., and J. M. Nerbonne. 1992. Two functionally distinct 4-aminopyridine sensitive outward K^+ currents in rat atrial myocytes. *The Journal of General Physiology.* 100:1041–1068.

Campbell, D. L., Y. Qu, R. L. Rasmusson, and H. C. Strauss. 1993. The calcium-independent transient outward potassium current in isolated ferret right ventricular myocytes. II. Closed state reverse use-dependent block by 4-aminopyridine. *Journal of General Physiology.* 101:603–626.

Chandy, K. G. 1991. Simplified gene nomenclature. *Nature.* 352:26.

Choi, K. L., R. W. Aldrich, and G. Yellen. 1991. Tetraethylammonium blockade distinguishes two inactivation mechanisms in voltage-activated K^+ channels. *Proceedings of the National Academy of Sciences, USA.* 88:5092–5095.

Chung, F.-Z., C. D. Wang, P. C. Potter, J. C. Venter, and C. M. Fraser. 1988. Site-directed mutagenesis and continuous expression of human β-adrenergic receptors. *The Journal of Biological Chemistry.* 263:4052–4055.

Demo, S. D., and G. Yellen. 1991. The inactivation gate of the Shaker K^+ channel behaves like an open channel blocker. *Neuron.* 7:743–753.

Durell, S. R., and H. R. Guy. 1992. Atomic scale structure and functional models of voltage-gated potassium channels. *Biophysical Journal.* 62:243–252.

Escande, D., A. Coulombe, J. F. Faivre, E. Deroubaix, and E. Coraboeuf. 1987. Two types of transient outward currents in adult human atrial cells. *American Journal of Physiology.* 252:H142–148.

Eyring, H., R. Lumry, and J. W. Woodbury. 1949. Some applications of modern rate theory in physiological systems. *Records of Chemical Progress.* 10:100–114.

Fan, Z., and M. Hiraoka. 1991. Depression of delayed outward K^+ current by Co^{2+} in guinea pig ventricular myocytes. *American Journal of Physiology.* 261:C23–31.

Folander, K., J. S. Smith, J. Antanavage, C. Bennett, R. B. Stein, and R. Swanson. 1990. Cloning and expression of the delayed-rectifier IsK channel from neonatal rat heart and diethylstilbestrol-primed rat uterus. *Proceedings of the National Academy of Sciences, USA.* 87:2975–2979.

Follmer, C. H., N. J. Lodge, C. A. Cullinan, and T. J. Colatsky. 1992. Modulation of the delayed rectifier, I_K, by cadmium in cat ventricular myocytes. *American Journal of Physiology.* 262:C75–83.

Frace, A. M., and J. J. Gargus. 1985. Activation of single-channel currents in mouse fibroblasts by platelet-derived growth factor. *Proceedings of the National Academy of Sciences, USA.* 86:2511–2515.

Gintant, G. A., I. S. Cohen, N. B. Datyner, and R. P. Kline. 1991. Time-dependent outward currents in the heart. *In* The Heart and Cardiovascular System: Scientific Foundations. H. A. Fozzard, E. Haber, R. B. Jennings, A. M. Katz, and H. E. Morgan, editors. Raven Press, New York. 1121–1169.

Goldman, D. E. 1943. Potential, impedance and rectification in membranes. *The Journal of General Physiology.* 27:37–60.

Hamill, O. P., A. Marty, E. Neher, B. Sakmann, and F. J. Sigworth. 1981. Improved patch clamp techniques for high-resolution current recording from cells and cell-free membrane patches. *Pflügers Archiv.* 391:85–100.

Heidbüchel, H., J. Vereecke, and E. Carmeliet. 1990. Three different potassium channels in human atrium: contribution to the basal potassium conductance. *Circulation Research.* 66:1277–1286.

Hille, B. 1991. Ionic Channels of Excitable Membranes. 2nd ed. Sinauer Associates, Inc., Sunderland, MA. 602 pp.

Hodgkin, A. L., and A. F. Huxley. 1952. A quantitative description of membrane current and its application to conduction and excitation in nerve. *The Journal of Physiology.* 117:500–544.

Hodgkin, A. L., and B. Katz. 1949. The effect of sodium ions on the electrical activity of the giant axon of the squid. *The Journal of Physiology.* 108:37–77.

Hoshi, T., W. N. Zagotta, and R. W. Aldrich. 1990. Biophysical and molecular mechanisms of *Shaker* potassium channel inactivation. *Science.* 250:533–538.

Hoshi, T., W. N. Zagotta, and R. W. Aldrich. 1991. Two type of inactivation in *Shaker* K^+ channels: effects of alterations in the carboxy-terminal region. *Neuron.* 7:547–556.

Hosoi, S., and C. L. Slayman. 1985. Membrane voltage, resistance, and channel switching in isolated mouse fibroblasts (L cells): a patch-electrode analysis. *The Journal of Physiology.* 367:267–290.

Hurst, R. S., A. E. Busch, M. P. Kavanaugh, P. B. Osborne, R. A. North, and J. P. Adelman. 1991. Identification of amino acids residues involved in dendrotoxin block of rat voltage-dependent potassium channels. *Molecular Pharmacology.* 40:572–576.

Imoto, K., C. Busch, B. Sakmann, M. Mishina, T. Konno, J. Nakai, H. Bujo, Y. Mori, K. Fukuda, and S. Numa. 1988. Rings of negatively charged amino acids determine the acetylcholine receptor channel conductance. *Nature.* 335:645–648.

Isacoff, E. Y., Y. N. Jan, and L. Y. Jan. 1991. Putative receptor for the cytoplasmic inactivation gate in the *Shaker* K^+ channel. *Nature.* 353:86–90.

Iverson, L. E., and B. Rudy. 1990. The role of the divergent amino and carboxyl domains on the inactivation properties of potassium channels derived from the *Shaker* gene of *Drosophila*. *Journal of Neuroscience.* 10:2903–2916.

Jeck, C. D., and P. A. Boyden. 1992. Age-related appearance of outward currents may contribute to developmental differences in ventricular repolarization. *Circulation Research.* 71:1390–1403.

Kass, R. S., T. Scheuer, and K. J. Malloy. 1982. Block of outward current in cardiac purkinje fibers by injection of quaternary ammonium ions. *The Journal of General Physiology.* 79:1041–1063.

Kavanaugh, M. P., M. D. Varnum, P. B. Osborne, M. J. Christie, A. E. Busch, J. P. Adelman, and R. A. North. 1991. Interaction between tetraethylammonium and amino acid residues in the pore of cloned voltage-dependent potassium channels. *The Journal of Biological Chemistry.* 266:7583–7587.

Kenyon, J. L., and W. R. Gibbons. 1978. 4-aminopyridine and the early outward current of sheep cardiac Purkinje fibers. *The Journal of General Physiology.* 73:139–157.

Koren, G., E. R. Liman, D. E. Logothetis, B. Nadal-Ginard, and P. Hess. 1990. Gating mechanism of a cloned potassium channel expressed in frog oocytes and mammalian cells. *Neuron.* 2:39–51.

Liman, E. R., J. Tytgat, and P. Hess. 1992. Subunit stoichiometry of a mammalian K^+ channel determined by construction of multimeric cDNAs. *Neuron.* 9:861–871.

MacKinnon, R. 1991. Determination of the subunit stoichiometry of a voltage-activated potassium channel. *Nature.* 350:232–235.

MacKinnon, R., and G. Yellen. 1990. Mutations affecting TEA blockade and ion permeation in voltage activated K^+ channels. *Science.* 250:276–279.

Matsubara, H., E. R. Liman, P. Hess, and G. Koren. 1992. Subunit stoichiometry of a mammalian K^+ channel determined by construction of multimeric cDNAs. *Neuron.* 9:861–871.

Matsuura, H., T. Ehara, and Y. Imoto. 1987. An analysis of the delayed outward current in single ventricular cells of the guinea-pig. *Pflügers Archiv.* 410:596–603.

Murai, T., A. Kakizuka, T. Takumi, H. Ohkubo, and S. Nakanishi. 1989. Molecular cloning and sequence analysis of human genomic DNA encoding a novel membrane protein which exhibits a slowly activating potassium channel activity. *Biochemical and Biophysical Research Communications.* 161:176–181.

Okada, Y., T. Yada, T. Ohno-Shosaku, and S. Oiki. 1986. Evidence for the involvement of calmodulin in the operation of Ca-activated K channels in mouse fibroblasts. *Journal of Membrane Biology.* 96:121–128.

Papazian, D. M., T. L. Schwarz, B. L. Tempel, Y. N. Jan, and L. Y. Jan. 1987. Cloning of genomic and complementary DNA from *Shaker,* a putative potassium channels gene from Drosophila. *Science.* 237:749–753.

Paulmichl, M., P. Nasmith, R. Hellmiss, K. Reed, W. A. Boyle, J. M. Nerbonne, E. G. Peralta, and D. E. Clapham. 1991. Cloning and expression of a rat delayed rectifier potassium channel. *Proceedings of the National Academy of Sciences, USA.* 88:7892–7895.

Perez-Reyes, E., H. S. Kim, A. E. Lacerda, W. Horne, X. Y. Wei, D. Rampe, K. P. Campbell, A. M. Brown, and L. Birnbaumer. 1989. Induction of calcium currents by the expression of the alpha 1-subunit of the dihydropyridine receptor from skeletal muscle. *Nature.* 340:233–236.

Pfaff, S. L., M. M. Tamkun, and W. L. Taylor. 1990. pOEV: a xenopus oocyte expression vector. *Analytical Biochemistry.* 188:192–199.

Philipson, L. H., R. E. Hice, K. Schaeffer, J. LaMendola, G. I. Bell, D. J. Nelson, and D. F. Steiner. 1991. Sequence and functional expression in *Xenopus* oocytes of a human insulinoma and islet potassium channel. *Proceedings of the National Academy of Sciences, USA.* 88:53–57.

Roberds, S. L., and M. M. Tamkun. 1991*a*. Cloning and tissue-specific expression of five voltage-gated potassium channel cDNAs expressed in rat heart. *Proceedings of the National Academy of Sciences, USA.* 88:1798–1802.

Roberds, S. L., and M. M. Tamkun. 1991*b*. Developmental expression of cloned cardiac potassium channels. *FEBS Letters.* 284:152–154.

Ruppersberg, J. P., R. Frank, O. Pongs, and M. Stocker. 1991. Cloned neuronal I_A channels reopen during recovery from inactivation. *Nature.* 353:657–660.

Sanguinetti, M. C., and N. K. Jurkiewicz. 1990*a*. Two components of cardiac delayed rectifier K^+ current. Differential sensitivity to block by class III antiarrhythmic agents. *The Journal of General Physiology.* 96:195–215.

Sanguinetti, M. C., and N. K. Jurkiewicz. 1990*b*. Lanthanum blocks a specific component of I_K and screens membrane surface charge in cardiac cells. *American Journal of Physiology.* 259:H1881–1889.

Shibata, E. F., T. Drury, H. Refsum, V. Aldrette, and W. R. Giles. 1989. Contributions of a transient outward current to repolarization in human atrium. *American Journal of Physiology.* 257:H1773–1781.

Snyders, D. J., P. B. Bennett, and L. M. Hondeghem. 1991*a*. Mechanisms of drug-channel interactions. *In* The Heart and Cardiovascular System: Scientific Foundations. H. A. Fozzard, E. Haber, R. B. Jennings, A. M. Katz, and H. E. Morgan, editors. Raven Press, New York. 2165–2193.

Snyders, D. J., F. A. Fish, S. L. Roberds, K. M. Knoth, M. M. Tamkun, and P. B. Bennett. 1991*b*. Stable exogenous expression of K^+ channels cloned from the mammalian cardiovascular system in mouse *Ltk*$^-$ cells. *Circulation.* 84:II-444. (Abstr.)

Snyders, D. J., and L. M. Hondeghem. 1990. Effects of quinidine on the sodium current of ventricular guinea-pig myocytes: evidence for a drug-associated rested state with altered kinetics. *Circulation Research.* 66:565–579.

Snyders, D. J., and B. G. Katzung. 1985. Clofilium reduces the plateau potassium current in isolated cardiac myocytes. *Circulation.* 72:III-233. (Abstr.)

Snyders, D. J., K. M. Knoth, S. L. Roberds, and M. M. Tamkun. 1991*c*. Stable mammalian expression of a human cardiac K^+ channel. *Circulation.* 84:II-103. (Abstr.)

Snyders, D. J., K. M. Knoth, S. L. Roberds, and M. M. Tamkun. 1992*a*. Time-, state- and voltage-dependent block by quinidine of a cloned human cardiac channel. *Molecular Pharmacology.* 41:332–339.

Snyders, D. J., S. L. Roberds, K. M. Knoth, P. B. Bennett, and M. M. Tamkun. 1992*b*. Block of a cloned human cardiac delayed rectifier by class III antiarrhythmic agents. *Biophysical Journal.* 61:151*a*. (Abstr.)

Spires, S., and T. Begenisich. 1989. Pharmacological and kinetic analysis of K channel gating currents. *The Journal of General Physiology.* 93:263–283.

Stühmer, W., M. Stocker, B. Sakmann, P. Seeburg, A. Baumann, A. Grupe, and O. Pongs. 1988. Potassium channels expressed from rat brain cDNA have delayed rectifier properties. *FEBS Letters.* 242:199–206.

Sutton, F., N. Davidson, and H. A. Lester. 1987. Tetrodotoxin-sensitive voltage-dependent Na currents recorded from *Xenopus* oocytes injected with mammalian cardiac muscle mRNA. *Molecular Brain Research.* 3:187–192.

Swanson, R., J. Marshall, J. S. Smith, J. B. Williams, M. B. Boyle, K. Folander, C. J. Luneau, J. Antanavage, C. Oliva, S. A. Buhrow et al. 1990. Cloning and expression of cDNA and genomic clones encoding three delayed rectifier potassium channels in rat brain. *Neuron.* 4:929–939.

Takeyasu, K., M. M. Tamkun, N. R. Siegel, and D. M. Fambrough. 1987. Expression of hybrid (Na^+K^+)-ATPase molecules after transfection of mouse *Ltk*$^-$ cells with DNA encoding the β subunit of an avian brain sodium pump. *The Journal of Biological Chemistry.* 262:10733–10740.

Takumi, T., H. Ohkubo, and S. Nakanishi. 1988. Cloning of a membrane protein that induces a slow voltage-gated potassium current. *Science.* 242:1042–1045.

Tamkun, M. M., K. M. Knoth, J. A. Walbridge, H. Kroemer, D. M. Roden, and D. M. Glover. 1991. Molecular cloning and characterization of two voltage-gated K^+ channel cDNAs from human ventricle. *FASEB Journal.* 5:331–337.

Thornhill, W. B., and S. R. Levinson. 1987. Biosynthesis of electroplax sodium channels in *Electrophorus* electrocytes and *Xenopus* oocytes. *Biochemistry.* 26:4381–4388.

Tseng-Crank, J. C., G. N. Tseng, A. Schwartz, and M. A. Tanouye. 1990. Molecular cloning and functional expression of a potassium channel cDNA isolated from a rat cardiac library. *FEBS Letters.* 268:63–68.

Ukomadu, C., J. Zhou, F. J. Sigworth, and W. S. Agnew. 1992. μI Na^+ channels expressed transiently in human embryonic kidney cells: biochemical and biophysical properties. *Neuron.* 8:663–676.

Van Bogaert, P. P., and D. J. Snyders. 1982. Effects of 4-aminopyridine on inward rectifying and pacemaker currents of cardiac Purkinje fibers. *Pflügers Archiv.* 394:230–238.

VanDongen, A. M. J., G. C. Frech, J. A. Drewe, R. H. Joho, and A. M. Brown. 1990. Alteration and restoration of K^+ channel function by deletions at the N- and C-termini. *Neuron.* 5:433–443.

Varadi, G., P. Lory, D. Schultz, M. Varadi, and A. Schwartz. 1991. Acceleration of activation and inactivation by the beta subunit of the skeletal muscle calcium channel. *Nature.* 352:159–162.

White, M. M., and F. Bezanilla. 1985. Activation of squid axon K^+ channels. Ionic and gating current studies. *The Journal of General Physiology.* 85:539–554.

Yeh, J. Z., G. S. Oxford, C. H. Wu, and T. Narahashi. 1976. Dynamics of aminopyridine block of potassium channels in squid axon membrane. *The Journal of General Physiology.* 68:519–535.

Yool, A. J., and T. L. Schwarz. 1991. Alterations of ionic selectivity of a K^+ channel by mutation of the H5 region. *Nature.* 349:700–704.

Yue, D. T., and E. Marban. 1988. A novel cardiac potassium channel that is active and conductive at depolarized potentials. *Pflügers Archiv.* 413:127–133.

Zagotta, W. N., and R. W. Aldrich. 1990. Voltage-dependent gating of *Shaker* A-type potassium channels in *Drosophila* muscle. *The Journal of General Physiology.* 95:29–60.